HHS Public Access

Author manuscript

Biochim Biophys Acta Mol Cell Res. Author manuscript; available in PMC 2023 January 23.

Published in final edited form as:

Biochim Biophys Acta Mol Cell Res. 2023 January ; 1870(1): 119386. doi:10.1016/j.bbamcr.2022.119386.

Impaired autophagic flux and dedifferentiation in podocytes lacking Asah1 gene: Role of lysosomal TRPML1 channel

Guangbi Li[a], **Dandan Huang**[a], **Yao Zou**[a], **Jason Kidd**[b], **Todd W.B. Gehr**[b], **Ningjun Li**[a], **Joseph K. Ritter**[a], **Pin-Lan Li**[a,*]

[a]Department of Pharmacology and Toxicology, School of Medicine, Virginia Commonwealth University, Richmond, VA, USA

[b]Division of Nephrology, School of Medicine, Virginia Commonwealth University, Richmond, VA, USA

Abstract

Podocytopathy and associated nephrotic syndrome have been reported in a mouse strain (Asah1$^{fl/fl}$/Podo^{cre}) with a podocyte-specific deletion of α subunit (the main catalytic subunit) of acid ceramidase (Ac). However, the pathogenesis of podocytopathy in these mice remains unclear. The present study tested whether Ac deficiency impairs autophagic flux in podocytes through blockade of transient receptor potential mucolipin 1 (TRPML1) channel as a potential pathogenic mechanism of podocytopathy in Asah1 $^{fl/fl}$/Podo^{cre} mice. We first demonstrated that impairment of autophagic flux occurred in podocytes lacking Asah1 gene, which was evidenced by autophagosome accumulation and reduced lysosome-autophagosome interaction. TRPML1 channel agonists recovered lysosome-autophagosome interaction and attenuated autophagosome accumulation in podocytes from Asah1$^{fl/fl}$/Podo^{cre} mice, while TRPML1 channel inhibitors impaired autophagic flux in WT/WT podocytes and worsened autophagic deficiency in podocytes lacking Asah1 gene. The effects of TRPML1 channel agonist were blocked by dynein inhibitors, indicating a critical role of dynein activity in the control of lysosome movement due to TRPML1 channel-mediated Ca^{2+} release. It was also found that there is an enhanced phenotypic transition to dedifferentiation status in podocytes lacking Asah1 gene in vitro and in vivo. Such podocyte phenotypic transition was inhibited by TRPML1 channel agonists but enhanced by TRPML1 channel inhibitors. Moreover, we found that TRPML1 gene silencing induced autophagosome accumulation and dedifferentiation in podocytes. Based on these results, we conclude that Ac activity is essential for autophagic flux and maintenance of differentiated status of podocytes. Dysfunction or deficiency of Ac may impair autophagic flux and induce

*Corresponding author at: Department of Pharmacology and Toxicology, Virginia Commonwealth University, School of Medicine, 1220 East Broad Street, Richmond, VA 23298-0613, USA. pin-lan.li@vcuhealth.org (P.-L. Li).

CRediT authorship contribution statement

Guangbi Li: Conceptualization, Methodology, Formal analysis, Investigation, Writing – original draft, Visualization. **Dandan Huang:** Formal analysis, Investigation. **Yao Zou:** Formal analysis, Investigation. **Jason Kidd:** Writing – review & editing. **Todd W.B. Gehr:** Writing – review & editing. **Ningjun Li:** Writing – review & editing. **Joseph K. Ritter:** Writing – review & editing. **Pin-Lan Li:** Conceptualization, Resources, Writing – review & editing, Supervision, Funding acquisition.

Declaration of competing interest

None of the authors have conflict of interest.

Appendix A. Supplementary data

Supplementary data to this article can be found online at https://doi.org/10.1016/j.bbamcr.2022.119386.

podocyte dedifferentiation, which may be an important pathogenic mechanism of podocytopathy and associated nephrotic syndrome.

Keywords

Podocyte; Lysosome; Autophagy; Dedifferentiation; Acid ceramidase; TRPML1 channel

1. Introduction

Since podocytes are terminally differentiated epithelial cells covering the outer surface of the glomerular capillaries, podocyte injury and dysfunction are not associated with podocyte proliferation in most glomerular diseases [1,2]. In these long-lived and non-proliferative podocytes, autophagy plays a vital role in the maintenance of their structural and functional integrity by degradation of various unnecessary or dysfunctional cellular components [3]. The process of autophagy includes initiation, elongation, maturation, fusion, and degradation [4,5]. The lysosome-autophagosome fusion to form autophagolysosomes and consequent lysosomal enzyme-dependent degradation of autophagosome cargos are defined as autophagic flux, which determines the degradation rate of autophagosomes [6]. It has been recognized that the normal function of lysosome is essential for podocytes through its effect on regulating autophagic flux [7,8]. Under pathological conditions, lysosome dysfunction and associated autophagic flux derangement have been shown to contribute to the development of podocytopathies and chronic glomerular diseases [9–11]. There is increasing evidence that impairment of autophagic flux can induce dedifferentiation, also known as epithelial-to-mesenchymal transition of podocytes in response to different pathological stimuli [12–16], indicating that dedifferentiation due to autophagic deficiency is a potential molecular mechanism mediating podocyte dysfunction.

Our recent studies have demonstrated an important role of acid ceramidase (Ac), a lysosomal enzyme which hydrolyzes ceramide into sphingosine and fatty acids, in the maintenance of structural and functional integrity of podocytes [17,18]. Mice with podocyte-specific knockout of Ac gene ($Asah1^{fl/fl}/Podo^{cre}$, Asah1 is mouse code of Ac gene) exhibited severe podocytopathy and associated nephrotic syndrome. Mechanistically, Ac deficiency leads to the inhibition of transient receptor potential mucolipin 1 (TRPML1) channel-mediated Ca^{2+} release in murine podocytes [18,19]. The blockade of TRPML1 channel activity decreased the interaction of lysosome and multivesicular body (MVB) thereby increasing exosome release in podocytes lacking Asah1 gene [18], demonstrating the importance of lysosomal TRPML1 channel in podocyte lysosome function. Indeed, enhanced exosome secretion from podocytes may be a biomarker of podocyte injury under pathological conditions [18,20–24]. These podocyte-derived exosomes might induce or enhance glomerular injury given that damaged podocyte-derived exosomes have been reported to induce renal tubular epithelial cell injury [25,26]. However, the pathogenic mechanism of podocytopathy due to Ac deficiency remains poorly understood. Considering the essential role of autophagy in the maintenance of structural and functional integrity of podocytes, testing whether autophagic deficiency in podocytes contributes to the pathogenesis of podocytopathy in $Asah1^{fl/fl}/Podo^{cre}$ mice would be of clinical interest.

In the present study, we tested the hypothesis that Ac deficiency impairs autophagic flux in podocytes due to reduced TRPML1 channel activity and thereby lead to podocytopathy in Asah1$^{fl/fl}$/Podo^{cre} mice. To test this hypothesis, we first examined whether lysosome-autophagosome fusion and lysosome-dependent degradation of autophagosome were interrupted in podocytes from Asah1$^{fl/fl}$/Podo^{cre} mice. Then, we determined the effects of TRPML1 channel agonists and TRPML1 channel inhibitors on autophagic flux and the role of a family of cytoskeletal motor protein, dynein in lysosome trafficking and lysosome-autophagosome interaction in podocytes. We also tested whether podocyte dedifferentiation occurred in Asah1$^{fl/fl}$/Podo^{cre} mice. Finally, we tested whether TRPML1 channel was involved in podocyte dedifferentiation due to Ac deficiency. Our results demonstrate that normal function of Ac is essential for autophagic flux and maintenance of differentiated status of podocytes. Dysfunction or deficiency of Ac may impair autophagic flux and induce podocyte dedifferentiation, which may contribute to the initiation and progression of podocytopathy and associated nephrotic syndrome.

2. Materials and methods

2.1. Animals

Podocyte-specific Cre recombinase (Podo^{cre}) mice were obtained from the Jackson Laboratory, Bar Harbor, Maine (B6.Cg-Tg(NPHS2-Cre) 295Lbh/J, stock number 008205). The mice carrying the floxed Ac α subunit construct were obtained from Erich Gulbins, University of Duisburg-Essen, Essen, Germany. The Asah1$^{fl/fl}$/Podo^{cre} mice and their littermates were on a C57/Bl6 background. Four-week-old WT/WT mice and Asah1$^{fl/fl}$/Podo^{cre} mice received daily intraperitoneal injection of ML-SA5 (Glixx Laboratories, Hopkinton, MA, USA) at 2 mg/kg or ML-SI1 (MedChemExpress, Monmouth Junction, NJ, USA) at 20 mg/kg for 4 weeks [27]. Each mouse used in our studies was genotyped for the Asah1$^{fl/fl}$ gene and Cre recombinase gene to confirm podocyte-specific gene deletion of acid ceramidase α subunit before use in experiments [17].

2.2. Primary culture of murine podocytes

Primary culture of murine podocytes was performed as described in previous studies [18,28]. We infused 20 mL of dynabeads from the abdominal aorta below the renal artery at flow rate of 7.4 mL/min/g kidney. After infusion, kidneys were removed, decapsulated, and dissected. The cortex was minced into small pieces and digested with mixture of collagenase A (1 mg/mL) and deoxyribonuclease I (0.2 mg/mL) in Hanks' balanced salt solution at 37 °C for 20 mins with gentle agitation. The digested tissue was placed on 100 μM strainer and gently pressed with ice-cold medium. After washing the glomeruli with ice-cold PBS for 6 times, we resuspended the isolated glomeruli with beads into 5 mL medium and transfer them into the collagen I-coated culture flask. After 3 days of culture of isolated glomeruli, cellular outgrowths were detached with Trypsin-ethylenediaminetetraacetic acid solution and transferred to a glass tube. Then, the glass tube was placed onto magnetic particle concentrator for 1 min to remove the glomerular cores and dynabeads. The supernatant was passed through a 40 μm sieve to remove the remaining glomerular cores. The filtered podocytes were cultured in D-MEM/F-12 (1:1) containing 10 % fetal bovine serum (Cansera International, Canada) supplemented with 0.5 % Insulin–Transferrin–Selenium-A liquid

media supplement (Invitrogen), 100 U/mL penicillin, and 100 mg/mL streptomycin on a new collagen I-coated flask at 37 °C before use in experiments. ML-SA5 (1 μM) [27], ML-SI1 (20 μM) [29], ML1-SA1 (20 μM) [30,31], steroid 17β-estradiol methyl ether (EDME) (10 μM) [32], ML2-SA1 (10 μM) [33], SF-31 (10 μM) [34,35], erythro-9-(2-hydroxy-3-nonyl)adenine (EHNA) (30 μM) [36], ciliobrevin D (50 μM) [37], chloroquine (100 μM) [38], and bafilomycin A1 (100 nM) [38] were used to treat podocytes in the present study.

2.3. GCaMP3 Ca^{2+} imaging

At 18–24 h after nucleofection with GCaMP3-ML1, podocytes were used for experiments [18,19]. The fluorescence intensity at 470 nm (F470) was recorded with a digital camera (Nikon Diaphoto TMD Inverted Microscope). Metafluor imaging and analysis software were used to acquire, digitize and store the images for offline processing and statistical analysis (Universal Imaging, Bedford Hills, NY, USA). Lysosomal Ca^{2+} release was measured under a “low” external Ca^{2+} solution, which contained 145 mM NaCl, 5 mM KCl, 3 mM MgCl2, 10 mM glucose, 1 mM EGTA and 20 mM HEPES (pH 7.4). GPN (Cayman Chemical, Ann Arbor, MI, USA) was used as positive control to induce Ca^{2+} release from lysosomes in podocytes.

2.4. Super-resolution microscopy

After treatments followed by fixation, the cells were incubated with rabbit anti-LC3 antibody (1:100; Cell Signaling Technology, Danvers, MA, USA) and rat anti-Lamp-1 antibody (1:100; Santa Cruz Biotechnology, Dallas, TX, USA) overnight at 4 °C. After slides being washed, Alexa 488-labeled anti-rabbit secondary antibody (1:200; Life Technologies, CA, USA) and Alexa 594-labeled anti-rat secondary antibody (1:200; Life Technologies, CA, USA) were added to the cell slides and incubated for 1 h at room temperature. Slides were then washed, stained with DAPI, and mounted. A Nikon fluorescence microscope in the structured illumination microscopy (SIM) mode was used to obtain images. Image Pro Plus 6.0 software (Media Cybernetics, Bethesda, MD, USA) was employed to analyze colocalization, expressed as the Pearson correlation coefficient [28,39].

2.5. Dynamic analysis of lysosome movement in podocytes

Podocytes cultured in 35 mm dish were incubated with 100 mg/mL dextran–Alexa Fluor 555 (Thermo Fisher Scientific, Waltham, MA, USA) for 6 h. The confocal fluorescent microscopic recording was conducted with a confocal laser scanning microscope (Fluoview FV1000, Olympus, Japan). The fluorescent images for lysosomes in podocytes were continuously recorded at an excitation/emission (nm) of 555/565 by using XYT recording mode with a speed of 1 frame/10 s for 10 min. Lysosome tracking was performed in Image J using manual tracking plugin as described in previous studies [36,40]. Ten lysosomes were chosen at random for each cell. These lysosomes were then tracked manually, while the program calculated velocity of lysosome trafficking for each frame.

2.6. Western blot analysis

Western blot analysis was performed as described previously [12]. In brief, homogenates of podocytes were prepared using sucrose buffer containing protease inhibitors. After boiling

for 5 min at 95 °C in a 5× loading buffer, 20 μg of total proteins were subjected to SDS-PAGE, transferred onto a PVDF membrane, and blocked by solution with dry milk. Then, the membrane was probed with primary antibodies of anti-ZO-1 (1:1000; Invitrogen, Waltham, MA, USA), anti-P-cadherin (1:1000; R&D, Minneapolis, MN, USA), anti-α-SMA (1:5000; R&D, Minneapolis, MN, USA), anti-FSP-1 (1:1000; Abcam Biotechnology, Cambridge, United Kingdom), or anti-β-actin (1:5000; Santa Cruz Biotechnology, Dallas, TX, USA) overnight at 4 °C followed by incubation with horseradish peroxidase-labeled IgG (1:5000). The immunoreactive bands were detected by chemiluminescence methods and visualized on Kodak Omat X-ray films. Densitometric analysis of the images obtained from X-ray films was performed using the Image J software (NIH, Bethesda, MD, USA).

2.7. Real-time reverse transcription polymerase chain reaction

Total RNA was isolated from podocytes of WT/WT and Asah1$^{fl/fl}$/Podo^{cre} mice, reversely transcribed to cDNA, and subjected to PCR amplification according to the procedures described previously [41]. Primers were synthesized by OriGene (Rockville, MD, USA) with the following sequences: Cdh3 (gene code of P-cadherin), sense CCAGACAAGGAGGACCAGAAGA and antisense CAAACTGCTCGTCCTCACGATC; S100a4 (gene code of FSP-1), sense AGCTCAAGGAG CTACTGACCAG and antisense GCTGTCCAAGTTGCTCATCACC.

2.8. Immunofluorescence microscopy

Immunofluorescence staining was performed using cultured podocytes grown on collagen-coated glass cover slips and frozen mouse kidney sections as described previously [42]. Briefly, after fixation the cells were incubated with rat anti-ZO-1 (1:100; Santa Cruz Biotechnology, Dallas, TX, USA) or rabbit anti-FSP-1 (1:100; Abcam Biotechnology, Cambridge, United Kingdom) overnight at 4 °C. Then, Alexa 488-labeled donkey anti-goat secondary antibody (1:200; Life Technologies, CA, USA) or Alexa 555-labeled donkey anti-rabbit secondary antibody (1:200; Life Technologies, CA, USA) was added to the cell slides and incubated for 1 h at room temperature. Slides were then washed, mounted, and observed using a confocal laser scanning microscope (Fluoview FV1000, Olympus, Japan).

2.9. Flow cytometric detection of autophagosomes

As described in previous studies [8,43], autophagosomes in podocytes were detected using a CytoID Autophagy Detection Kit (Enzo, Plymouth Meeting, PA, USA). The CytoID fluorescent reagents specifically detect the autophagic vacuoles formed during autophagy. Briefly, cells were trypsinized, spun down, and washed twice in phenol red-free RPMI 1640 with 2 % foetal bovine serum (FBS). The cells were resuspended in 0.5 mL of freshly diluted CytoID reagents and incubated at 37 °C for 30 min. The CytoID fluorescence of cells was immediately analysed by flow cytometry using a flow cytometer (GUAVA, Hayward, CA, USA). The percentage of cells with CytoID staining was used to represent the relative formation or accumulation of autophagosomes.

2.10. Statistical analysis

All the values are expressed as mean ± SEM. Significant differences among multiple groups were examined using ANOVA followed by a Student-Newman-Keuls test. $P < 0.05$ was considered statistically significant.

3. Results

3.1. Impaired autophagic flux in podocytes lacking Asah1 gene

We first tested whether autophagic deficiency occurred in podocytes lacking Asah1 gene. We stained podocytes of WT/WT and Asah1$^{fl/fl}$/Podo^{cre} mice with CYTO-ID probe to quantify autophagosomes in these cells by flow cytometry. Higher intracellular level of CYTO-ID green fluorescence indicates more autophagosomes in podocytes. In Fig. 1A, the x axis means the intracellular intensity of CYTO-ID green fluorescence; the y axis indicates the ratio of cells with various intensity of green fluorescence. The representative curves of flow cytometry indicated that autophagosome accumulation occurred in podocytes of Asah1$^{fl/fl}$/Podo^{cre} mice compared with WT/WT podocytes. Summarized data showed that the amount of autophagosomes was significantly increased by Asah1 gene deletion in podocytes, which was similar to the effect of chloroquine (CQ), an autophagy inhibitor (Fig. 1B). Also, we performed Western blot analysis to determine the ratio of LC3-II over LC3-I in podocytes. It was found that the levels of LC3-I were similar in podocytes of WT/WT and Asah1$^{fl/fl}$/Podo^{cre} mice. However, Ac deficiency remarkably increased LC3-II in podocytes and thereby led to significant elevation of LC3-II/LC3-I, indicating autophagosome accumulation in podocytes of Asah1$^{fl/fl}$/Podo^{cre} mice. Bafilomycin A1 (Baf), an autophagy inhibitor, had similar effects on LC3-II/LC3-I in podocytes (Fig. 1C and D). Since enhanced autophagosome biogenesis and reduced autophagosome degradation both can cause autophagosome accumulation, we observed lysosome-autophagosome interaction by superresolution microscopy to confirm whether autophagic flux was altered by Asah1 gene deletion. As shown in Fig. 1E, the encounter and fusion of autophagosome and lysosome and the formation of autophagolysosome were indicated by yellow dots in the cytosol of podocytes. In WT/WT podocytes, there was considerable number of yellow dots in the cytosol. In podocytes of Asah1$^{fl/fl}$/Podo^{cre} mice, however, the number of yellow dots in the cytosol dropped remarkably. Statistical analysis showed that the reduction of lysosome-autophagosome interaction by Asah1 gene knockout was significant, indicating deficient autophagic flux in podocytes lacking Asah1 gene (Fig. 1F).

3.2. Regulation of autophagic flux by lysosomal TRPML1 channel in podocytes

Since our recent studies have shown that Ac deficiency leads to inhibition of TRPML1 channel activity [18,19], we wondered whether TRPML1 channel is involved in the deficient autophagic flux due to Ac deficiency in podocytes. Recently, we have demonstrated that the expression of TRPML1 is remarkably higher than TRPML2 and TRPML3 in mouse glomeruli and podocytes [41]. To further confirm the dominant role of TRPML1 channel in lysosomal Ca^{2+} release in podocytes, we performed real-time RT-PCR and confocal microscopy on podocytes of WT/WT mice. As shown in Supplementary Fig. 1, real-time RT-PCR results showed that the mRNA level of TRPML1 was remarkably higher than TRPML2 and TRPML3 in WT/WT podocytes. By confocal microscopy, we

found that colocalization of TRPML1 and Lamp-1 was significantly higher than TRPML2 and TRPML3 in WT/WT podocytes, suggesting the abundant expression of TRPML1 in lysosomes of these cells. To specifically detect Ca^{2+} release through lysosomal TRPML1 channel, nucleofection of GCaMP3-ML1 plasmid into podocytes was performed to express GCaMP3, a single-wavelength genetically encoded Ca^{2+} indicator, on the cytoplasmic amino terminus of TRPML1 in these cells as described in our previous studies [18,19]. A fluorescent microscopic imaging system was used to dynamically and continuously monitor the GCaMP3 fluorescence signal (F470) in podocytes. The intensity of Ca^{2+}-induced GCaMP3 fluorescence indicated the amount of Ca^{2+} released through lysosomal TRPML1 channel. As shown in Fig. 2, both ML-SA5 (TRPML channel agonist) and ML1-SA1 (TRPML1 channel agonist) induced rapid elevations of GCaMP3 fluorescence in WT/WT podocytes, which was followed by a large signal increase caused by late addition of ionomycin, a Ca^{2+} ionophore. Also, ML-SA5 and ML1-SA1 induced smaller elevations of GCaMP3 fluorescence in podocytes of $Asah1^{fl/fl}/Podo^{cre}$ mice. Although summarized data showed that Ca^{2+} release through TRPML1 channel induced by ML-SA5 or ML1-SA1 was significantly attenuated by Asah1 gene deletion, our findings indicate that ML-SA5 and ML1-SA1 can partially overcome the inhibition of TRPML1 channel activity by Ac deficiency.

Then, we tested whether TRPML1 channel is implicated in the regulation of autophagic flux in podocytes. By super-resolution microscopy, we found that both ML-SA5 and ML1-SA1 significantly enhanced lysosome-autophagosome interaction in WT/WT podocytes compared with vehicle-treated cells. On the contrary, it was found that ML-SI1 (TRPML channel inhibitor) and EDME (TRPML1 channel inhibitor) obviously decreased the encounter and fusion of lysosome and autophagosome, leading to less formation of autophagolysosome in WT/WT podocytes. In podocytes of $Asah1^{fl/fl}/Podo^{cre}$ mice, impaired autophagic flux due to Ac deficiency was recovered by agonists but worsened by inhibitors (Fig. 3A and B). Also, we quantified autophagosomes in podocytes of different groups by flow cytometry. In WT/WT podocytes, the density of autophagosome in cytosol was unchanged by agonists but elevated by inhibitors. As the outcome of autophagic deficiency, autophagosome accumulation due to Ac deficiency was attenuated by ML-SA5 and ML1-SA1 but amplified by ML-SI1 and EDME in podocytes of $Asah1^{fl/fl}/Podo^{cre}$ mice (Fig. 3C and D). However, ML2-SA1 (TRPML2 channel agonist) and SF-31 (TRPML3 channel agonist) were found to have no effects on lysosome-autophagosome interaction in podocytes of both WT/WT and $Asah1^{fl/fl}/Podo^{cre}$ mice. Autophagosome accumulation in podocytes lacking Asah1 gene was unchanged by ML2-SA1 and SF-31.

3.3. Contribution of dynein activity to lysosome trafficking and autophagic flux in podocytes

Mechanistically, we tested the possibility that lysosome trafficking in response to TRPML1 channel-mediated Ca^{2+} release depends on the activity of dynein in podocytes. Dextran–Alexa Fluor 555 was loaded into live podocytes and the lysosome movement was continuously monitored for 10 min under different conditions. Fig. 4A showed the lysosome movement in a WT/WT podocyte after the activation of TRPML1 channel by ML-SA5. Summarized data showed that ML-SA5 significantly enhanced lysosome trafficking in

WT/WT podocytes compared with control cells. The impaired lysosome trafficking due to Ac deficiency was recovered by ML-SA5 in podocytes lacking Asah1 gene. Although, pre-treating podocytes of both WT/WT and Asah1$^{fl/fl}$/Podo^{cre} mice with dynein inhibitors, EHNA and ciliobrevin D, blocked the stimulating effect of ML-SA5 on lysosome movement in these cells (Fig. 4B).

Furthermore, we examined whether the activity of dynein is required for autophagic flux in podocytes. By structured illumination microscopy, decreased encounter and fusion of lysosome and autophagosome were observed in podocytes of Asah1$^{fl/fl}$/Podo^{cre} mice compared with WT/WT podocytes. The lysosome-autophagosome interaction was significantly enhanced by activation of TRPML1 channel by ML-SA5 in podocytes of both WT/WT and Asah1$^{fl/fl}$/Podo^{cre} mice. However, inhibition of dynein activity by EHNA and ciliobrevin D blocked the enhancive effect of ML-SA5 on lysosome-autophagosome interaction in these cells (Fig. 4C and D).

3.4. Podocyte dedifferentiation due to Asah1 gene deletion

To determine whether Asah1 gene knockout induces dedifferentiation in podocytes, Western blot analysis was performed to detect epithelial markers and mesenchymal markers in podocytes of WT/WT and Asah1$^{fl/fl}$/Podo^{cre} mice. We found that Asah1 gene knockout significantly inhibited the expression of epithelial markers, P-cadherin and ZO-1, in podocytes (Fig. 5A and B). On the contrary, the expression of FSP-1 and α-SMA as mesenchymal markers was remarkably enhanced by Ac deficiency in podocytes (Fig. 5C and D). Moreover, real-time RT-PCR was performed to detect mRNA levels of P-cadherin and FSP-1 in podocytes of WT/WT and Asah1$^{fl/fl}$/Podo^{cre} mice. It was found that mRNA of P-cadherin was significantly reduced in podocytes lacking Asah1 gene compared to WT/WT podocytes (Fig. 5E). In contrast, Asah1 gene deletion remarkably increased mRNA of FSP-1 in podocytes compared to control cells (Fig. 5F). Immunofluorescent staining was performed on frozen kidney slides of WT/WT and Asah1$^{fl/fl}$/Podo^{cre} mice for detection of epithelial markers and mesenchymal markers in glomeruli. As shown in Fig. 6, when Asah1 gene was deleted in podocytes, P-cadherin and ZO-1 as epithelial markers decreased obviously, while the mesenchymal markers FSP-1 and α-SMA increased remarkably. Statistical analysis showed that Ac deficiency-induced decline of epithelial markers and elevation of mesenchymal markers in glomeruli were significant.

3.5. Inhibition of dedifferentiation by enhancement of TRPML1 channel activity in podocytes lacking Asah1 gene

We also tested whether enhancement of TRPML1 channel activity inhibits podocyte dedifferentiation due to Ac deficiency. As shown in Fig. 7A and B, Asah1 gene deletion significantly decreased the expression of ZO-1, an epithelial marker, in podocytes of Asah1$^{fl/fl}$/Podo^{cre} mice compared with WT/WT podocytes. The activation of TRPML1 channel by ML-SA5 and ML1-SA1 attenuated the decline of ZO-1 in podocytes lacking Asah1 gene. Inhibition of TRPML1 channel activity by ML-SI1 and EDME, however, suppressed the expression of ZO-1 in WT/WT podocytes and worsened the reduction of ZO-1 in podocytes of Asah1$^{fl/fl}$/Podo^{cre} mice. In contrast, FSP-1 as a mesenchymal marker remarkably increased in podocytes lacking Asah1 gene compared with WT/WT podocytes.

This elevation was significantly inhibited by ML-SA5 and ML1-SA1. However, ML-SI1 and EDME enhanced the expression of FSP-1 in WT/WT podocytes and amplified the elevation of FSP-1 in podocytes of Asah1$^{fl/fl}$/Podo^{cre} mice via inhibition of TRPML1 channel activity (Fig. 7C and D). It was found that ML2-SA1 and SF-31 had no effects on the expressions of ZO-1 and FSP-1 in podocytes of both WT/WT and Asah1$^{fl/fl}$/Podo^{cre} mice.

Then, we treated WT/WT and Asah1$^{fl/fl}$/Podo^{cre} mice with vehicle, ML-SA5, or ML-SI1 to further confirm our findings in cell studies. It was found that podocyte-specific Asah1 gene deletion simultaneously decreased podocin, a podocyte slit diaphragm protein, and ZO-1 in glomeruli of Asah1$^{fl/fl}$/Podo^{cre} mice compared with WT/WT mice. These reductions due to Ac deficiency were both attenuated by the intraperitoneal injection of ML-SA5. On the contrary, the inhibition of TRPML1 channel activity by ML-SI1 decreased glomerular podocin and ZO-1 in WT/WT mice and worsened their reductions due to Ac deficiency in Asah1$^{fl/fl}$/Podo^{cre} mice (Fig. 8A-C). In addition, we found that decline of nephrin, a podocyte slit diaphragm protein, and elevation of α-SMA simultaneously occurred in glomeruli of Asah1$^{fl/fl}$/Podo^{cre} mice compared with WT/WT mice. These pathological changes due to podocyte-specific Asah1 gene deletion were significantly inhibited by ML-SA5. In contrast, the intraperitoneal injection of ML-SI1 induced reduction of nephrin and elevation of α-SMA in glomeruli of WT/WT mice and amplified these pathological changes in glomeruli of Asah1$^{fl/fl}$/Podo^{cre} mice (Fig. 8D-F). Moreover, urinary protein excretion was measured per 24 h in WT/WT and Asah1$^{fl/fl}$/Podo^{cre} mice in different groups. As shown in Fig. 9, severe proteinuria was found in Asah1$^{fl/fl}$/Podo^{cre} mice compared with WT/WT mice. The elevation of urinary protein excretion due to podocyte-specific Asah1 gene deletion was significantly attenuated by the intraperitoneal injection of ML-SA5. On the contrary, ML-SI1 elevated urinary protein excretion in WT/WT mice and worsened proteinuria in Asah1$^{fl/fl}$/Podo^{cre} mice.

3.6. Autophagosome accumulation and dedifferentiation in podocytes with TRPML1 gene silencing

To further confirm whether TRPML1 channel mediates the regulation of autophagy and differentiation by Ac in podocytes, we tested whether TRPML1 gene silencing affected autophagy and differentiation in podocytes. As shown in Supplementary Fig. 2, we performed Western blot analysis to confirm that TRPML1 shRNA remarkably decreased the expression of TRPML1 in WT/WT podocytes compared to cells transfected with scramble shRNA. By CytoID flow cytometry, we demonstrated that the amount of autophagosomes was significantly increased in WT/WT podocytes transfected with TRPML1 shRNA compared to cells transfected with scramble shRNA (Fig. 10A and B). Moreover, we detected ZO-1 and FSP-1 levels in podocytes by immunofluorescent staining. It was found that WT/WT podocytes transfected with TRPML1 shRNA had decreased ZO-1 expression and increased FSP-1 expression compared to control cells (Fig. 10C and D).

4. Discussion

The major goal of the present study was to determine whether Ac deficiency impairs autophagic flux in podocytes through blockade of TRPML1 channel and to test

whether Asah1 gene deletion-induced podocyte dedifferentiation can be attenuated by enhancement of TRPML1 channel activity in mice. It was found that Ac deficiency due to podocyte-specific Asah1 gene deletion interrupted lysosome-autophagosome interaction and lysosomal enzyme-dependent degradation of autophagosome, which was attenuated by TRPML1 channel agonists, but worsened by TRPML1 channel inhibitors. We also demonstrated that lysosome trafficking in response to TRPML1 channel activation depended on dynein, a microtubule motor protein. Furthermore, we observed podocyte dedifferentiation in Asah1$^{fl/fl}$/Podo^{cre} mice, which was diminished by TRPML1 channel agonists, but aggravated by TRPML1 channel inhibitors, indicating the contribution of blockade of TRPML1 channel and consequent autophagic flux deficiency to podocyte dedifferentiation. These results suggest that Ac-TRPML1-dynein signaling pathway controls autophagic flux in podocytes, which is essential for the maintenance of structural and functional integrity of these cells.

It has been reported that mutations in the AC gene or deficiency of lysosomal AC activity in human cells is a major genetic or pathogenic mechanism for the development of Farber disease, which features hoarseness and painful swollen joints accompanied by nephropathy with elevated urine ceramide levels as characteristic features [44]. A recent study has shown that the normal function of lysosomal Ac is essential for the protection of podocytes from oxidative stress and apoptosis under pathologic conditions [45]. More recently, we have demonstrated that podocyte-specific Asah1 gene deletion may induce podocytopathy and nephrotic syndrome in mice [17]. Although, the underlying pathogenic mechanism remains poorly understood. Given the important role of autophagy in the maintenance of podocyte homeostasis [7–11], we tested whether Asah1 gene knockout-induced podocytopathy is attributed to deficient autophagic flux in the present study. In podocytes isolated from WT/WT and Asah1$^{fl/fl}$/Podo^{cre} mice, we demonstrated that Asah1 gene knockout induced autophagosome accumulation, indicating impairment of autophagic flux. Importantly, Ac deficiency was found to interrupt lysosome-autophagosome interaction in podocytes of Asah1$^{fl/fl}$/Podo^{cre} mice. These findings together confirm that Asah1 gene deletion-induced autophagosome accumulation is attributed to lysosome dysfunction, but not abnormal autophagosome biogenesis. To our knowledge, these results represent the first experimental evidence that normal function of Ac is essential for autophagic flux in podocytes. In this regard, the overexpression of Ac has been reported to enhance autophagy and resistance to C6 ceramide in prostate cancer cells [46], while the ablation of Ac impairs autophagy and mitochondria activity in melanoma cells [47]. However, the molecular mechanism mediating the regulatory role of Ac in autophagy has not been elucidated in these previous studies.

As a cation channel, TRPML1 channel is mainly expressed on lysosomes and late endosomes [48]. There is increasing evidence that various cellular activities are controlled by TRPML1 channel [49]. As a key process of autophagy, the fusion of lysosome and autophagosome is mediated by TRPML1 channel [50–52]. In addition, it has been found that TRPML1 channel activity contributes to autophagosome biogenesis, which may be due to the induction of the Beclin1/VPS34 autophagic complex, the activation of calcium/calmodulin-dependent protein kinase kinase β, the boost of AMP-activated protein kinase, and the generation of phosphatidylinositol 3-phosphate [53]. Recent studies have demonstrated that the normal function of TRPML1 channels is essential for the

maintenance of renal glomerular homeostasis and thereby involved in the development of some glomerular diseases. In podocytes, lysosomal Ca^{2+} release through TRPML1 channel has been reported to contribute to lysosome trafficking and lysosome-MVB interaction and thereby control MVB fate and exosome release [18,19,39]. Moreover, it has been reported that Ac-dependent sphingolipid metabolism regulates TRPML1 channel activity in podocytes [18,19]. Given the important role of TRPML1 channel activity in autophagic flux, we hypothesized that Asah1 gene deletion-induced deficiency of autophagic flux may be associated with the inhibition of TRPML1 channel activity. The present study demonstrated that activation of TRPML1 channel by TRPML1 channel agonists recovered lysosome-autophagosome interaction and attenuated autophagosome accumulation in podocytes. On the contrary, the blockade of TRPML1 channel by TRPML1 channel inhibitors mimicked the effect of Asah1 gene knockout on autophagic flux. Moreover, TRPML1 channel inhibitors enhanced the impairment of autophagic flux due to Ac deficiency. Consistently, autophagosome accumulation has been found in fibroblasts patients with mucolipidosis type IV, a lysosomal storage disease due to mutations in Mucolipin 1 [51]. Moreover, it has been reported that up-regulation of lysosomal TRPML1 channel is essential for lysosomal adaptation to nutrient starvation, indicating the contribution of TRPML1 channel to autophagic flux [54]. Although these previous studies showed the implication of TRPML1 channel in the regulation of autophagic flux, the results from the present study for the first time demonstrate that Ac-dependent activation of TRPML1 channels can increase lysosome-autophagosome fusion leading to enhancement of autophagic flux.

The present study further examined the molecular mechanism by which TRPML1 channel regulates lysosome-autophagosome interaction in autophagic flux. There is increasing evidence that lysosomes respond to the environmental changes by actively trafficking towards their targets, such as phagosome, autophagosome, and MVB [55,56]. Previous studies have shown that lysosome trafficking depends on motor proteins, such as dynein, dynactin, and kinesin-1 [57]. It has been reported that lysosomal Ca^{2+} release through TRPML1 channel activates the cytosolic calcium sensor ALG2 to recruit the dynein/dynactin complex, leading to lysosome trafficking towards the perinuclear region [58]. Therefore, we tested whether dynein activity is required for lysosome trafficking in response to TRPML1 channel activation in podocytes. In the present study, we confirmed that dynein inhibitors EHNA and ciliobrevin D prevented the enhancement of lysosome trafficking by ML-SA5 by observing lysosome movement in live podocytes. Furthermore, we demonstrated that the elevation of lysosome-autophagosome fusion by ML-SA5 was blocked by EHNA and ciliobrevin D. These data imply that dynein importantly controls lysosome trafficking in response to TRPML1 channel activation and thereby determine autophagic flux in podocytes. In previous studies, dynein has been reported to participate in autophagosome movement for lysosome-autophagosome fusion in HeLa cells [59], glioma cells [60], and mouse coronary arterial myocytes [36]. However, it remained unknown whether dynein can affect lysosome trafficking to regulate autophagic flux. Our findings together with previous studies have revealed that dynein may regulate the movement of both autophagosome and lysosome to fine control the autophagic flux for the maintenance of cellular homeostasis.

In addition to degradation of various unnecessary or dysfunctional cellular components, autophagy has been reported to participate in cell differentiation by controlling the fate of transcription factor complexes and their regulators [61]. Meanwhile, autophagic deficiency is implicated in cell dedifferentiation under different pathological conditions [62]. In podocytes, impaired autophagic flux due to inhibition of lysosome function has been reported to induce dedifferentiation [12]. In diabetic nephropathy, autophagic deficiency contributes to the development of podocyte dedifferentiation [13] and enhancement of autophagy attenuates podocyte dedifferentiation [14,15]. The disrupted apolipoprotein L1-miR193a axis-induced podocyte dedifferentiation is also attributed to autophagic deficiency [16]. The present study tested whether Asah1 gene deletion-induced autophagic deficiency leads to dedifferentiation in podocytes. It was demonstrated that dedifferentiation occurred in podocytes lacking Asah1 gene, which was evidenced by decreased epithelial markers and increased mesenchymal markers in podocytes of $Asah1^{fl/fl}/Podo^{cre}$ mice, as shown in both cell and animal studies. Our findings support the view that podocyte dedifferentiation serve as a pathogenic mechanism of podocytopathy and nephrotic syndrome in $Asah1^{fl/fl}/Podo^{cre}$ mice.

To confirm the role of impaired autophagic flux in podocyte dedifferentiation in $Asah1^{fl/fl}/Podo^{cre}$ mice, we tested whether TRPML1 channel agonists and inhibitors can alter differentiation status of podocytes in vitro and in vivo. In the cell studies, we demonstrated that reduction of epithelial marker and elevation of mesenchymal marker due to Asah1 gene knockout were blocked by TRPML1 channel agonists but amplified by TRPML1 channel inhibitors. In animal studies, treatment with ML-SA5 not only inhibited the changes in epithelial marker and mesenchymal marker, but also attenuated the decline of slit diaphragm proteins and proteinuria in $Asah1^{fl/fl}/Podo^{cre}$ mice. Inhibition of TRPML1 channel by ML-SI1, however, had the opposite effects on epithelial marker, mesenchymal marker, slit diaphragm proteins, and urinary protein excretion. These results suggest that inhibition of TRPML1 channel due to Asah1 gene deletion contributes to the enhancement of podocyte dedifferentiation in $Asah1^{fl/fl}/Podo^{cre}$ mice. Although previous studies have revealed that TRPML1 channel may regulate lysosome trafficking and thereby control exosome release in podocytes [18,19,39], it remained unknown whether TRPML1 channel is involved in the regulation of structure and function of podocytes. The present study answered this question, indicating that the normal function of TRPML1 channel is essential for the maintenance of differentiation status of podocytes.

Mucolipidosis type IV (MLIV) is an autosomal recessive neurodegenerative lysosomal storage disorder caused by mutations in the gene (MCOLN1 for human and Mcoln1 for mouse) encoding mucolipin-1 (TRPML1) [63]. It has been reported that the fusion of lysosome and autophagosome is inhibited in fibroblasts of MLIV patients [51]. Moreover, TRPML1 channel was found to contribute to lysosome-autophagosome interaction [50–52]. Based on these previous studies, we also tested whether TRPML1 gene silencing can affect autophagic flux in podocytes. It was found that TRPML shRNA induced autophagosome accumulation and dedifferentiation in podocytes, suggesting that normal expression of TRPML1 gene is indispensable for autophagic flux and maintenance of differentiation status of podocytes. These findings further confirmed the vital role of TRPML1 channel in the regulation of autophagic flux in podocytes. In this regard, Ca^{2+}

released through TRPML1 channel was found to activate calcineurin which is responsible for the dephosphorylation of TFEB. Then, dephosphorylated TFEB translocated to nucleus to initiate the transcription of lysosomal and autophagic genes [64,65]. Recently, it has been found that TRPML1 contributes to autophagosome biogenesis, which is attributed to the induction of the Beclin1/VPS34 autophagic complex, the activation of calcium/calmodulin-dependent protein kinase kinase β (CaMKKβ), the boost of AMP-activated protein kinase (AMPK), and the generation of phosphatidylinositol 3-phosphate (PI3P) [53]. Moreover, there is increasing evidence showing that boost of autophagy may be attributed to production of reactive oxygen species (ROS), which is a vital defensive mechanism against cellular stress [66,67]. Under conditions such as ischemia, hypoxia, and nutrient starvation, autophagy may be induced by mitochondrial ROS [68–70]. Nevertheless, autophagosome accumulation was observed after induction of autophagy by ROS [71–73], indicating that lysosome-dependent autophagosome degradation may be interfered. Recently, we have demonstrated that endogenously produced ROS may impair TRPML1 channel activity and thereby inhibit lysosome-dependent MVB degradation, leading to enhanced inflammatory exosome release from podocytes [39]. Together, these findings suggest that TRPML1 channel plays a significant role in the regulation of autophagy in podocytes under various physiological and pathological conditions.

5. Conclusions

The present study demonstrated that lysosomal Ac participated in the maintenance of differentiated status of podocytes. Asah1 gene knockout impaired autophagic flux and induced dedifferentiation in podocytes, which was associated with inhibition of TRPML1 channel activity. These results indicate that impaired autophagic flux and consequent enhancement of podocyte dedifferentiation during Ac deficiency may serve as an important pathogenic mechanism of podocytopathy and associated nephrotic syndrome and that Ac and TRPML1 channel could be a new therapeutic target for prevention or treatment of nephrotic syndrome due to podocytopathy.

Supplementary Material

Refer to Web version on PubMed Central for supplementary material.

Acknowledgements

The GCaMP3-ML1 plasmid was kindly provided by Dr. Haoxing Xu (Department of Molecular, Cellular, and Developmental Biology, University of Michigan, Ann Arbor, MI). The TRPML1 channel agonist, ML1-SA1, was kindly provided by Dr. Christian Grimm (Walther Straub Institute of Pharmacology and Toxicology, Ludwig-Maximilians-University, Munich, Germany).

Funding

This study was supported by grants DK054927 and DK120491 from National Institutes of Health.

Data availability

Data will be made available on request.

References

[1]. Mundel P, Shankland SJ, Podocyte biology and response to injury, J. Am. Soc. Nephrol 13 (2002) 3005–3015. [PubMed: 12444221]

[2]. Pavenstadt H, Kriz W, Kretzler M, Cell biology of the glomerular podocyte, Physiol. Rev 83 (2003) 253–307. [PubMed: 12506131]

[3]. Li G, Kidd J, Li PL, Podocyte lysosome dysfunction in chronic glomerular diseases, Int. J. Mol. Sci 21 (2020).

[4]. Sun K, Deng W, Zhang S, Cai N, Jiao S, Song J, Wei L, Paradoxical roles of autophagy in different stages of tumorigenesis: protector for normal or cancer cells, Cell Biosci. 3 (2013) 35. [PubMed: 24016776]

[5]. Glick D, Barth S, Macleod KF, Autophagy: cellular and molecular mechanisms, J. Pathol 221 (2010) 3–12. [PubMed: 20225336]

[6]. Loos B, du Toit A, Hofmeyr JH, Defining and measuring autophagosome flux-concept and reality, Autophagy 10 (2014) 2087–2096. [PubMed: 25484088]

[7]. Liu WJ, Gan Y, Huang WF, Wu HL, Zhang XQ, Zheng HJ, Liu HF, Lysosome restoration to activate podocyte autophagy: a new therapeutic strategy for diabetic kidney disease, Cell Death Dis. 10 (2019) 806. [PubMed: 31649253]

[8]. Xiong J, Xia M, Xu M, Zhang Y, Abais JM, Li G, Riebling CR, Ritter JK, Boini KM, Li PL, Autophagy maturation associated with CD38-mediated regulation of lysosome function in mouse glomerular podocytes, J. Cell. Mol. Med 17 (2013) 1598–1607. [PubMed: 24238063]

[9]. Liu WJ, Li ZH, Chen XC, Zhao XL, Zhong Z, Yang C, Wu HL, An N, Li WY, Liu HF, Blockage of the lysosome-dependent autophagic pathway contributes to complement membrane attack complex-induced podocyte injury in idiopathic membranous nephropathy, Sci. Rep 7 (2017) 8643. [PubMed: 28819100]

[10]. Hou B, Li Y, Li X, Zhang C, Zhao Z, Chen Q, Zhang N, Li H, HGF protected against diabetic nephropathy via autophagy-lysosome pathway in podocyte by modulating PI3K/Akt-GSK3beta-TFEB axis, Cell. Signal 75 (2020), 109744. [PubMed: 32827692]

[11]. Yamamoto-Nonaka K, Koike M, Asanuma K, Takagi M, Oliva Trejo JA, Seki T, Hidaka T, Ichimura K, Sakai T, Tada N, Ueno T, Uchiyama Y, Tomino Y, Cathepsin D, Podocytes is important in the pathogenesis of proteinuria and CKD, J. Am. Soc. Nephrol 27 (2016) 2685–2700. [PubMed: 26823550]

[12]. Li G, Li CX, Xia M, Ritter JK, Gehr TW, Boini K, Li PL, Enhanced epithelial-to-mesenchymal transition associated with lysosome dysfunction in podocytes: role of p62/Sequestosome 1 as a signaling hub, Cell. Physiol. Biochem 35 (2015) 1773–1786. [PubMed: 25832774]

[13]. Jin J, Wu D, Zhao L, Zou W, Shen W, Tu Q, He Q, Effect of autophagy and stromal interaction molecule 1 on podocyte epithelial-mesenchymal transition in diabetic nephropathy, Int. J. Clin. Exp. Pathol 11 (2018) 2450–2459. [PubMed: 31938357]

[14]. Tu Q, Li Y, Jin J, Jiang X, Ren Y, He Q, Curcumin alleviates diabetic nephropathy via inhibiting podocyte mesenchymal transdifferentiation and inducing autophagy in rats and MPC5 cells, Pharm. Biol 57 (2019) 778–786. [PubMed: 31741405]

[15]. Tao M, Zheng D, Liang X, Wu D, Hu K, Jin J, He Q, Tripterygium glycoside suppresses epithelialtomesenchymal transition of diabetic kidney disease podocytes by targeting autophagy through the mTOR/Twist1 pathway, Mol. Med. Rep 24 (2021).

[16]. Kumar V, Ayasolla K, Jha A, Mishra A, Vashistha H, Lan X, Qayyum M, Chinnapaka S, Purohit R, Mikulak J, Saleem MA, Malhotra A, Skorecki K, Singhal PC, Disrupted apolipoprotein L1-miR193a axis dedifferentiates podocytes through autophagy blockade in an APOL1 risk milieu, Am J Physiol Cell Physiol 317 (2019) C209–C225. [PubMed: 31116585]

[17]. Li G, Kidd J, Kaspar C, Dempsey S, Bhat OM, Camus S, Ritter JK, Gehr TWB, Gulbins E, Li PL, Podocytopathy and nephrotic syndrome in mice with podocyte-specific deletion of the Asah1 gene: role of ceramide accumulation in glomeruli, Am. J. Pathol 190 (2020) 1211–1223. [PubMed: 32194052]

[18]. Li G, Huang D, Bhat OM, Poklis JL, Zhang A, Zou Y, Kidd J, Gehr TWB, Li PL, Abnormal podocyte TRPML1 channel activity and exosome release in mice with podocyte-specific Asah1

gene deletion, Biochim. Biophys. Acta Mol. Cell Biol. Lipids 1866 (2021), 158856. [PubMed: 33221496]

[19]. Li G, Huang D, Hong J, Bhat OM, Yuan X, Li PL, Control of lysosomal TRPML1 channel activity and exosome release by acid ceramidase in mouse podocytes, Am J Physiol Cell Physiol 317 (2019) C481–C491. [PubMed: 31268777]

[20]. Spanu S, van Roeyen CR, Denecke B, Floege J, Muhlfeld AS, Urinary exosomes: a novel means to non-invasively assess changes in renal gene and protein expression, PLoS One 9 (2014), e109631. [PubMed: 25310591]

[21]. Zhou H, Kajiyama H, Tsuji T, Hu X, Leelahavanichkul A, Vento S, Frank R, Kopp JB, Trachtman H, Star RA, Yuen PS, Urinary exosomal Wilms' tumor-1 as a potential biomarker for podocyte injury, Am. J. Physiol. Renal Physiol 305 (2013) F553–F559. [PubMed: 23761678]

[22]. Kalani A, Mohan A, Godbole MM, Bhatia E, Gupta A, Sharma RK, Tiwari S, Wilm's tumor-1 protein levels in urinary exosomes from diabetic patients with or without proteinuria, PLoS One 8 (2013), e60177. [PubMed: 23544132]

[23]. Zhou H, Cheruvanky A, Hu X, Matsumoto T, Hiramatsu N, Cho ME, Berger A, Leelahavanichkul A, Doi K, Chawla LS, Illei GG, Kopp JB, Balow JE, Austin HA 3rd, Yuen PS, Star RA, Urinary exosomal transcription factors, a new class of biomarkers for renal disease, Kidney Int. 74 (2008) 613–621. [PubMed: 18509321]

[24]. Lv LL, Cao YH, Pan MM, Liu H, Tang RN, Ma KL, Chen PS, Liu BC, CD2AP mRNA in urinary exosome as biomarker of kidney disease, Clin. Chim. Acta 428 (2014) 26–31. [PubMed: 24144866]

[25]. Jeon JS, Kim E, Bae YU, Yang WM, Lee H, Kim H, Noh H, Han DC, Ryu S, Kwon SH, microRNA in extracellular vesicles released by damaged podocytes promote apoptosis of renal tubular epithelial cells, Cells 9 (2020).

[26]. Su H, Qiao J, Hu J, Li Y, Lin J, Yu Q, Zhen J, Ma Q, Wang Q, Lv Z, Wang R, Podocyte-derived extracellular vesicles mediate renal proximal tubule cells dedifferentiation via microRNA-221 in diabetic nephropathy, Mol. Cell. Endocrinol 518 (2020), 111034. [PubMed: 32926967]

[27]. Yu L, Zhang X, Yang Y, Li D, Tang K, Zhao Z, He W, Wang C, Sahoo N, Converso-Baran K, Davis CS, Brooks SV, Bigot A, Calvo R, Martinez NJ, Southall N, Hu X, Marugan J, Ferrer M, Xu H, Small-molecule activation of lysosomal TRP channels ameliorates Duchenne muscular dystrophy in mouse models, Sci. Adv 6 (2020), eaaz2736. [PubMed: 32128386]

[28]. Huang D, Li G, Bhat OM, Zou Y, Li N, Ritter JK, Li PL, Exosome biogenesis and lysosome function determine podocyte exosome release and glomerular inflammatory response during hyperhomocysteinemia, Am. J. Pathol 192 (2022) 43–55. [PubMed: 34717894]

[29]. Leser C, Keller M, Gerndt S, Urban N, Chen CC, Schaefer M, Grimm C, Bracher F, Chemical and pharmacological characterization of the TRPML calcium channel blockers ML-SI1 and ML-SI3, Eur. J. Med. Chem 210 (2021), 112966. [PubMed: 33187805]

[30]. Spix B, Butz ES, Chen CC, Rosato AS, Tang R, Jeridi A, Kudrina V, Plesch E, Wartenberg P, Arlt E, Briukhovetska D, Ansari M, Gunsel GG, Conlon TM, Wyatt A, Wetzel S, Teupser D, Holdt LM, Ectors F, Boekhoff I, Boehm U, Garcia-Anoveros J, Saftig P, Giera M, Kobold S, Schiller HB, Zierler S, Gudermann T, Wahl-Schott C, Bracher F, Yildirim AO, Biel M, Grimm C, Lung emphysema and impaired macrophage elastase clearance in mucolipin 3 deficient mice, Nat. Commun 13 (2022) 318. [PubMed: 35031603]

[31]. Siow WX, Kabiri Y, Tang R, Chao YK, Plesch E, Eberhagen C, Flenkenthaler F, Frohlich T, Bracher F, Grimm C, Biel M, Zischka H, Vollmar AM, Bartel K, Lysosomal TRPML1 regulates mitochondrial function in hepatocellular carcinoma cells, J. Cell Sci 135 (2022).

[32]. Ruhl P, Rosato AS, Urban N, Gerndt S, Tang R, Abrahamian C, Leser C, Sheng J, Jha A, Vollmer G, Schaefer M, Bracher F, Grimm C, Estradiol analogs attenuate autophagy, cell migration and invasion by direct and selective inhibition of TRPML1, independent of estrogen receptors, Sci. Rep 11 (2021) 8313. [PubMed: 33859333]

[33]. Plesch E, Chen CC, Butz E, Scotto Rosato A, Krogsaeter EK, Yinan H, Bartel K, Keller M, Robaa D, Teupser D, Holdt LM, Vollmar AM, Sippl W, Puertollano R, Medina D, Biel M, Wahl-Schott C, Bracher F, Grimm C, Selective agonist of TRPML2 reveals direct role in chemokine release from innate immune cells, eLife 7 (2018).

[34]. Saldanha SA, Grimm C, Allais C, Smith E, Ouizem S, Mercer BA, Roush WR, Heller S, Hodder P, Identification of selective agonists of the transient receptor potential channels 3 (TRPML3), in: Probe Reports From the NIH Molecular Libraries Program, Bethesda (MD), 2010.

[35]. Grimm C, Jors S, Saldanha SA, Obukhov AG, Pan B, Oshima K, Cuajungco MP, Chase P, Hodder P, Heller S, Small molecule activators of TRPML3, Chemistry & biology 17 (2010) 135–148. [PubMed: 20189104]

[36]. Xu M, Li XX, Xiong J, Xia M, Gulbins E, Zhang Y, Li PL, Regulation of autophagic flux by dynein-mediated autophagosomes trafficking in mouse coronary arterial myocytes, Biochim. Biophys. Acta 2013 (1833) 3228–3236.

[37]. Firestone AJ, Weinger JS, Maldonado M, Barlan K, Langston LD, O'Donnell M, Gelfand VI, Kapoor TM, Chen JK, Small-molecule inhibitors of the AAA+ ATPase motor cytoplasmic dynein, Nature 484 (2012) 125–129. [PubMed: 22425997]

[38]. Mauthe M, Orhon I, Rocchi C, Zhou X, Luhr M, Hijlkema KJ, Coppes RP, Engedal N, Mari M, Reggiori F, Chloroquine inhibits autophagic flux by decreasing autophagosome-lysosome fusion, Autophagy 14 (2018) 1435–1455. [PubMed: 29940786]

[39]. Li G, Huang D, Li N, Ritter JK, Li PL, Regulation of TRPML1 channel activity and inflammatory exosome release by endogenously produced reactive oxygen species in mouse podocytes, Redox Biol. 43 (2021), 102013. [PubMed: 34030116]

[40]. Jahreiss L, Menzies FM, Rubinsztein DC, The itinerary of autophagosomes: from peripheral formation to kiss-and-run fusion with lysosomes, Traffic 9 (2008) 574–587. [PubMed: 18182013]

[41]. Li G, Huang D, Hong J, Bhat OM, Yuan X, Li PL, Control of lysosomal TRPML1 channel activity and exosome release by acid ceramidase in mouse podocytes, Am. J. Physiol. Cell Physiol 317 (2019) C481–C491. [PubMed: 31268777]

[42]. Li G, Zhang Q, Hong J, Ritter JK, Li PL, Inhibition of pannexin-1 channel activity by adiponectin in podocytes: role of acid ceramidase activation, Biochim. Biophys. Acta Mol. Cell Biol. Lipids 2018 (1863) 1246–1256.

[43]. Zhang Y, Xu M, Xia M, Li X, Boini KM, Wang M, Gulbins E, Ratz PH, Li PL, Defective autophagosome trafficking contributes to impaired autophagic flux in coronary arterial myocytes lacking CD38 gene, Cardiovasc. Res 102 (2014) 68–78. [PubMed: 24445604]

[44]. Park JH, Schuchman EH, Acid ceramidase and human disease, Biochim. Biophys. Acta 1758 (2006) 2133–2138. [PubMed: 17064658]

[45]. Choi SR, Lim JH, Kim MY, Kim EN, Kim Y, Choi BS, Kim YS, Kim HW, Lim KM, Kim MJ, Park CW, Adiponectin receptor agonist AdipoRon decreased ceramide, and lipotoxicity, and ameliorated diabetic nephropathy, Metabolism 85 (2018) 348–360. [PubMed: 29462574]

[46]. Turner LS, Cheng JC, Beckham TH, Keane TE, Norris JS, Liu X, Autophagy is increased in prostate cancer cells overexpressing acid ceramidase and enhances resistance to C6 ceramide, Prostate Cancer Prostatic Dis. 14 (2011) 30–37. [PubMed: 21116286]

[47]. Lai M, La Rocca V, Amato R, Freer G, Costa M, Spezia PG, Quaranta P, Lombardo G, Piomelli D, Pistello M, Ablation of acid ceramidase impairs autophagy and mitochondria activity in melanoma cells, Int. J. Mol. Sci 22 (2021).

[48]. Sun M, Goldin E, Stahl S, Falardeau JL, Kennedy JC, Acierno JS Jr., Bove C, Kaneski CR, Nagle J, Bromley MC, Colman M, Schiffmann R, Slaugenhaupt SA, Mucolipidosis type IV is caused by mutations in a gene encoding a novel transient receptor potential channel, Hum. Mol. Genet 9 (2000) 2471–2478. [PubMed: 11030752]

[49]. Cheng X, Shen D, Samie M, Xu H, Mucolipins: intracellular TRPML1-3 channels, FEBS Lett. 584 (2010) 2013–2021. [PubMed: 20074572]

[50]. Venkatachalam K, Wong CO, Zhu MX, The role of TRPMLs in endolysosomal trafficking and function, Cell Calcium 58 (2015) 48–56. [PubMed: 25465891]

[51]. Vergarajauregui S, Connelly PS, Daniels MP, Puertollano R, Autophagic dysfunction in mucolipidosis type IV patients, Hum. Mol. Genet 17 (2008) 2723–2737. [PubMed: 18550655]

[52]. Ahuja M, Park S, Shin DM, Muallem S, TRPML1 as lysosomal fusion guard, Channels 10 (2016) 261–263. [PubMed: 27028119]

[53]. Scotto Rosato A, Montefusco S, Soldati C, Di Paola S, Capuozzo A, Monfregola J, Polishchuk E, Amabile A, Grimm C, Lombardo A, De Matteis MA, Ballabio A, Medina DL, TRPML1

links lysosomal calcium to autophagosome biogenesis through the activation of the CaMKKbeta/VPS34 pathway, Nat. Commun 10 (2019) 5630. [PubMed: 31822666]

[54]. Wang W, Gao Q, Yang M, Zhang X, Yu L, Lawas M, Li X, Bryant-Genevier M, Southall NT, Marugan J, Ferrer M, Xu H, Up-regulation of lysosomal TRPML1 channels is essential for lysosomal adaptation to nutrient starvation, Proc. Natl. Acad. Sci. U. S. A 112 (2015) E1373–E1381. [PubMed: 25733853]

[55]. Grimm C, Butz E, Chen CC, Wahl-Schott C, Biel M, From mucolipidosis type IV to ebola: TRPML and two-pore channels at the crossroads of endo-lysosomal trafficking and disease, Cell Calcium 67 (2017) 148–155. [PubMed: 28457591]

[56]. Saftig P, Klumperman J, Lysosome biogenesis and lysosomal membrane proteins: trafficking meets function, Nat. Rev. Mol. Cell Biol 10 (2009) 623–635. [PubMed: 19672277]

[57]. Cabukusta B, Neefjes J, Mechanisms of lysosomal positioning and movement, Traffic 19 (2018) 761–769. [PubMed: 29900632]

[58]. Li X, Rydzewski N, Hider A, Zhang X, Yang J, Wang W, Gao Q, Cheng X, Xu H, A molecular mechanism to regulate lysosome motility for lysosome positioning and tubulation, Nat. Cell Biol 18 (2016) 404–417. [PubMed: 26950892]

[59]. Kimura S, Noda T, Yoshimori T, Dynein-dependent movement of autophagosomes mediates efficient encounters with lysosomes, Cell Struct. Funct 33 (2008) 109–122. [PubMed: 18388399]

[60]. Yamamoto M, Suzuki SO, Himeno M, The effects of dynein inhibition on the autophagic pathway in glioma cells, Neuropathology 30 (2010) 1–6. [PubMed: 19496938]

[61]. Clarke AJ, Simon AK, Autophagy in the renewal, differentiation and homeostasis of immune cells, Nat. Rev. Immunol 19 (2019) 170–183. [PubMed: 30531943]

[62]. Chen HT, Liu H, Mao MJ, Tan Y, Mo XQ, Meng XJ, Cao MT, Zhong CY, Liu Y, Shan H, Jiang GM, Crosstalk between autophagy and epithelial-mesenchymal transition and its application in cancer therapy, Mol. Cancer 18 (2019) 101. [PubMed: 31126310]

[63]. Pryor PR, Reimann F, Gribble FM, Luzio JP, Mucolipin-1 is a lysosomal membrane protein required for intracellular lactosylceramide traffic, Traffic 7 (2006) 1388–1398. [PubMed: 16978393]

[64]. Medina DL, Ballabio A, Lysosomal calcium regulates autophagy, Autophagy 11 (2015) 970–971. [PubMed: 26000950]

[65]. Medina DL, Di Paola S, Peluso I, Armani A, De Stefani D, Venditti R, Montefusco S, Scotto-Rosato A, Prezioso C, Forrester A, Settembre C, Wang W, Gao Q, Xu H, Sandri M, Rizzuto R, De Matteis MA, Ballabio A, Lysosomal calcium signalling regulates autophagy through calcineurin and TFEB, Nat. Cell Biol 17 (2015) 288–299. [PubMed: 25720963]

[66]. Scherz-Shouval R, Shvets E, Fass E, Shorer H, Gil L, Elazar Z, Reactive oxygen species are essential for autophagy and specifically regulate the activity of Atg4, EMBO J. 26 (2007) 1749–1760. [PubMed: 17347651]

[67]. Scherz-Shouval R, Elazar Z, Regulation of autophagy by ROS: physiology and pathology, Trends Biochem. Sci 36 (2011) 30–38. [PubMed: 20728362]

[68]. Filomeni G, De Zio D, Cecconi F, Oxidative stress and autophagy: the clash between damage and metabolic needs, Cell Death Differ. 22 (2015) 377–388. [PubMed: 25257172]

[69]. Mi Y, Xiao C, Du Q, Wu W, Qi G, Liu X, Momordin ic couples apoptosis with autophagy in human hepatoblastoma cancer cells by reactive oxygen species (ROS)-mediated PI3K/Akt and MAPK signaling pathways, Free Radic. Biol. Med 90 (2016) 230–242. [PubMed: 26593748]

[70]. Scherz-Shouval R, Shvets E, Elazar Z, Oxidation as a post-translational modification that regulates autophagy, Autophagy 3 (2007) 371–373. [PubMed: 17438362]

[71]. Zhang X, Cheng X, Yu L, Yang J, Calvo R, Patnaik S, Hu X, Gao Q, Yang M, Lawas M, Delling M, Marugan J, Ferrer M, Xu H, MCOLN1 is a ROS sensor in lysosomes that regulates autophagy, Nat. Commun 7 (2016) 12109. [PubMed: 27357649]

[72]. Kim RJ, Hah YS, Sung CM, Kang JR, Park HB, Do antioxidants inhibit oxidative-stress-induced autophagy of tenofibroblasts? J. Orthop. Res 32 (2014) 937–943. [PubMed: 24644146]

[73]. Liu GY, Jiang XX, Zhu X, He WY, Kuang YL, Ren K, Lin Y, Gou X, ROS activates JNK-mediated autophagy to counteract apoptosis in mouse mesenchymal stem cells in vitro, Acta Pharmacol. Sin 36 (2015) 1473–1479. [PubMed: 26592514]

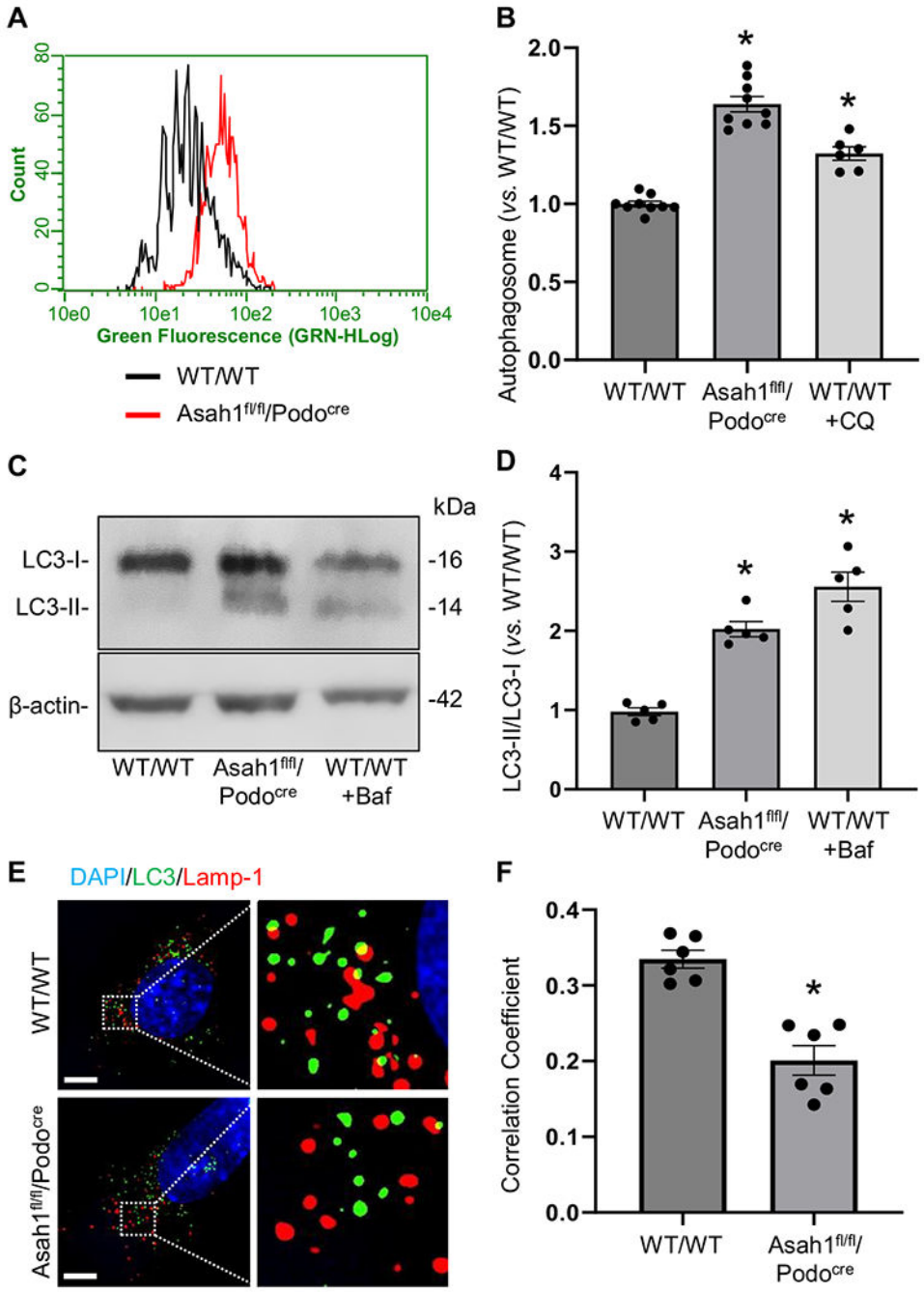

Fig. 1.

Impaired autophagic flux in podocytes lacking Asah1 gene. A. Representative curves showing the ratio of podocytes of WT/WT and Asah1$^{fl/fl}$/Podo^{cre} mice with different density of autophagosome. B. Summarized data showing that Asah1 gene deletion and CQ significantly increased autophagosomes in podocytes (n = 6–9). C. Representative gel documents showing the expression of LC3-I and LC3-II in WT/WT podocytes, podocytes lacking Asah1 gene, and Baf-treated WT/WT podocytes. D. Summarized data showing that Asah1 gene knockout and Baf significantly elevated the ratio of LC3-II over LC3-I

in podocytes ($n = 5$). E. Representative images showing that Asah1 gene deletion reduced lysosome-autophagosome interaction in podocytes. Scale bars = 5 μm. F. Summarized data showing that lysosome-autophagosome interaction was significantly inhibited in podocytes lacking Asah1 gene (n = 6). * $P < 0.05$ vs. WT/WT group.

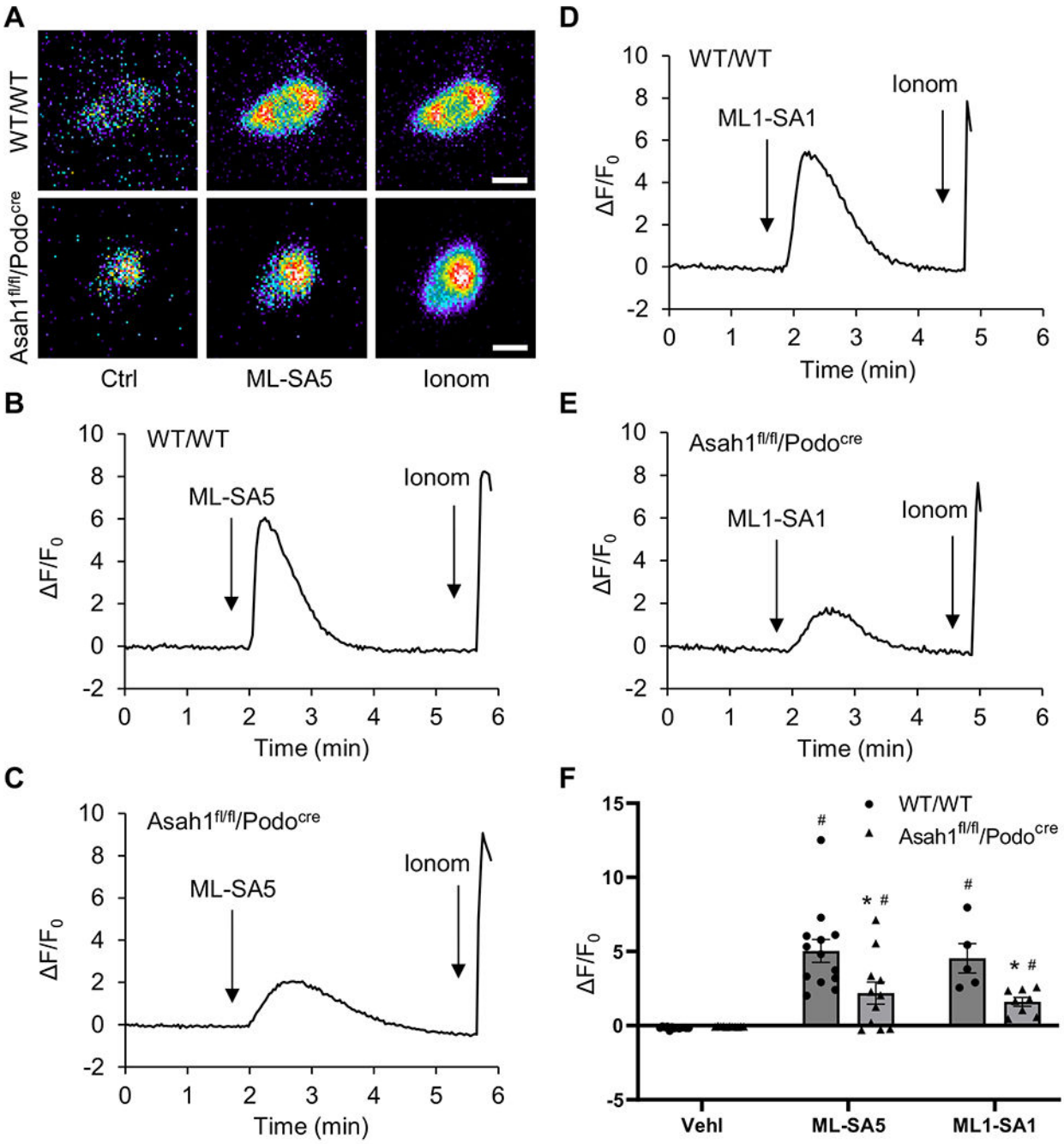

Fig. 2.

Partial activation of TRPML1 channel by ML-SA5 and ML1-SA1 in podocytes lacking Asah1 gene. A. Representative images showing that Ac deficiency inhibited TRPML1 channel-mediated Ca^{2+} release induced by ML-SA5 in podocytes. Scale bars = 40 μm. B. A representative curve showing that ML-SA5 induced elevation of GCaMP3 signal in podocytes of WT/WT mice. C. A representative curve showing that ML-SA5 induced smaller elevation of GCaMP3 signal in podocytes lacking Asah1 gene compared with WT/WT podocytes. D. A representative curve showing that ML1-SA1 induced elevation

of GCaMP3 signal in podocytes of WT/WT mice. E. A representative curve showing that ML1-SA1 induced smaller elevation of GCaMP3 signal in podocytes lacking Asah1 gene compared with WT/WT podocytes. F. Summarized data showing that Asah1 gene knockout significantly attenuated TRPML1-mediated Ca^{2+} release induced by ML-SA5 or ML1-SA1 in podocytes (n = 5–13). * $p < 0.05$ vs. WT/WT group, # $p < 0.05$ vs. Vehl group. Ctrl, control; Ionom, ionomycin; Vehl, vehicle.

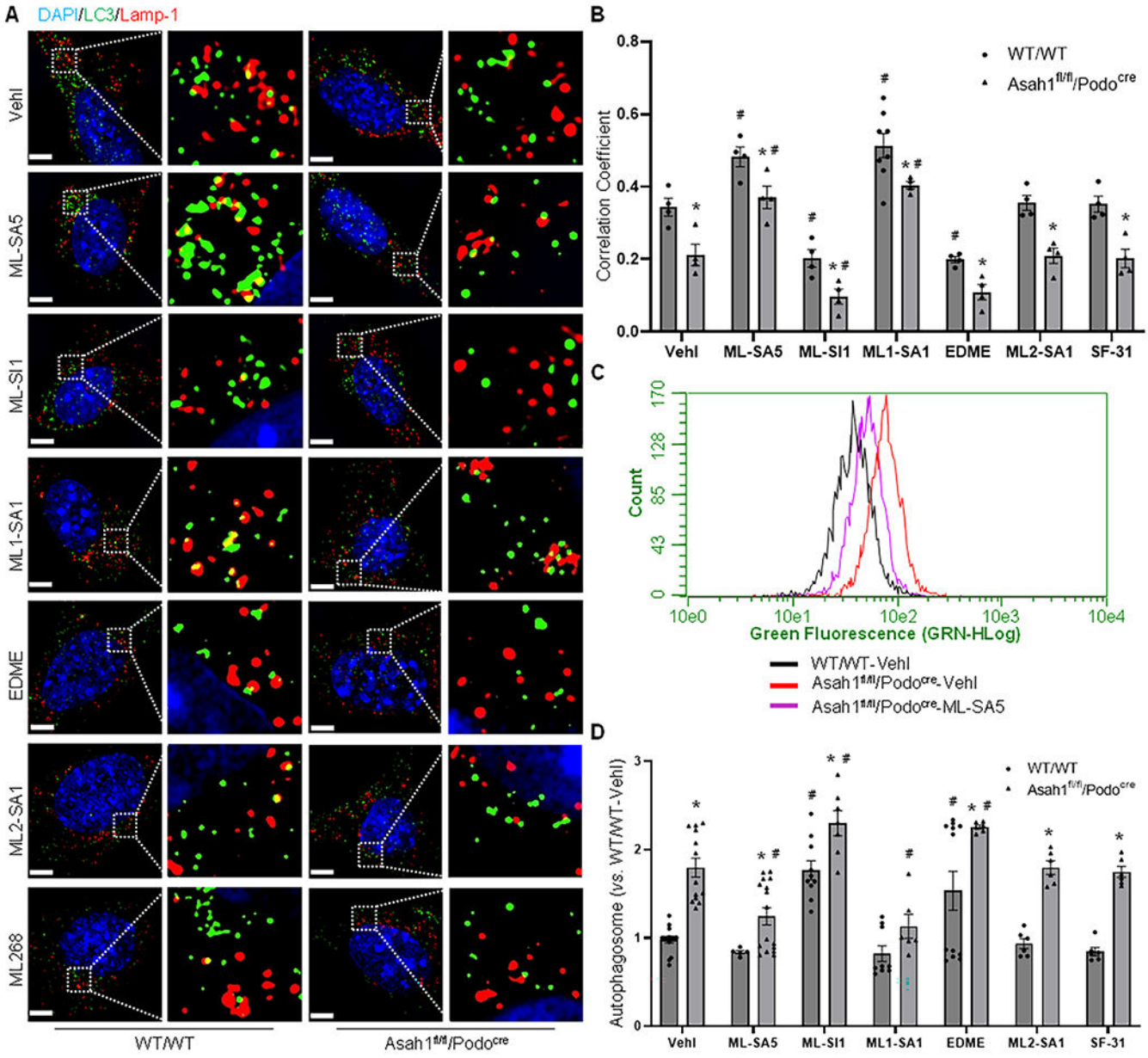

Fig. 3.

Regulation of autophagic flux by lysosomal TRPML1 channel in podocytes. A. Representative images showing lysosome-autophagosome interaction in podocytes of WT/WT and Asah1$^{fl/fl}$/Podo^{cre} mice under different conditions. Scale bars = 5 μm. B. Summarized data showing lysosome-autophagosome interaction in podocytes of WT/WT and Asah1$^{fl/fl}$/Podo^{cre} mice under different conditions (n = 4–8). C. Representative curves showing the ratio of podocytes of WT/WT and Asah1$^{fl/fl}$/Podo^{cre} mice under different conditions with different density of autophagosome. D. Summarized data showing autophagosome density in podocytes of WT/WT and Asah1$^{fl/fl}$/Podo^{cre} mice under different conditions (n = 5–16). * P < 0.05 vs. WT/WT group. # P < 0.05 vs. Vehl group.

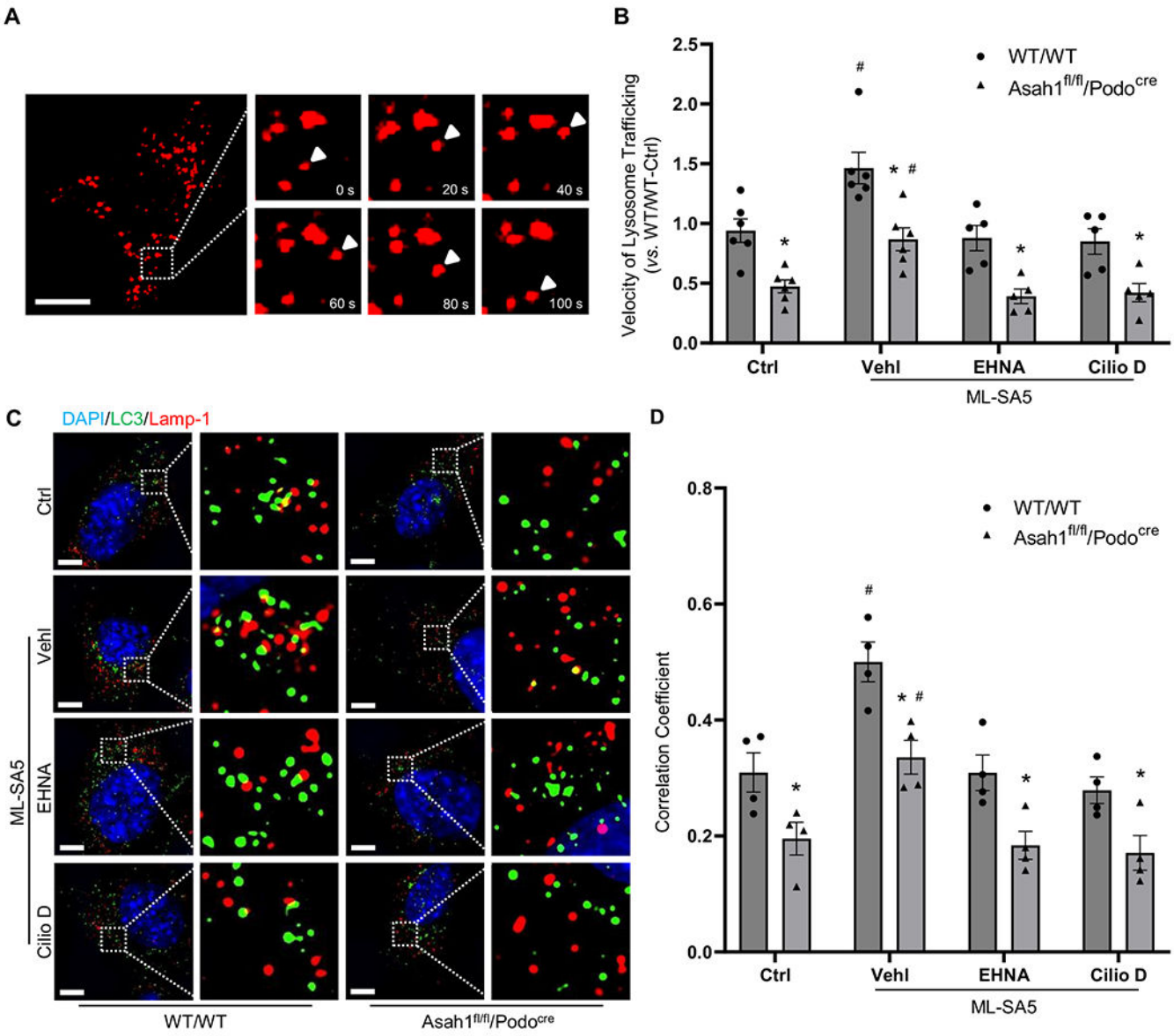

Fig. 4.

Contribution of dynein activity to lysosome trafficking and autophagic flux in podocytes. A. Representative images showing the lysosome movement in a WT/WT podocyte after the activation of TRPML1 channel by ML-SA5. Scale bars = 20 μm. B. Summarized data showing velocity of lysosome trafficking in podocytes of WT/WT and Asah1$^{fl/fl}$/Podo^{cre} mice under different conditions. Asah1 gene deletion, EHNA, and ciliobrevin D significantly decreased velocity of lysosome trafficking in podocytes. ML-SA5 significantly increased velocity of lysosome trafficking in podocytes (n = 5–6). C. Representative images showing lysosome-autophagosome interaction in podocytes of WT/WT and Asah1$^{fl/fl}$/Podo^{cre} mice under different conditions. Scale bars = 5 μm. D. Summarized data showing lysosome-autophagosome interaction in podocytes of WT/WT and Asah1$^{fl/fl}$/Podo^{cre} mice under different conditions. Asah1 gene deletion, EHNA, and ciliobrevin D significantly inhibited lysosome-autophagosome interaction in podocytes. ML-SA5

significantly enhanced lysosome-autophagosome interaction in podocytes ($n = 4$). * $P < 0.05$ vs. WT/WT group. # P < 0.05 vs. Ctrl group.

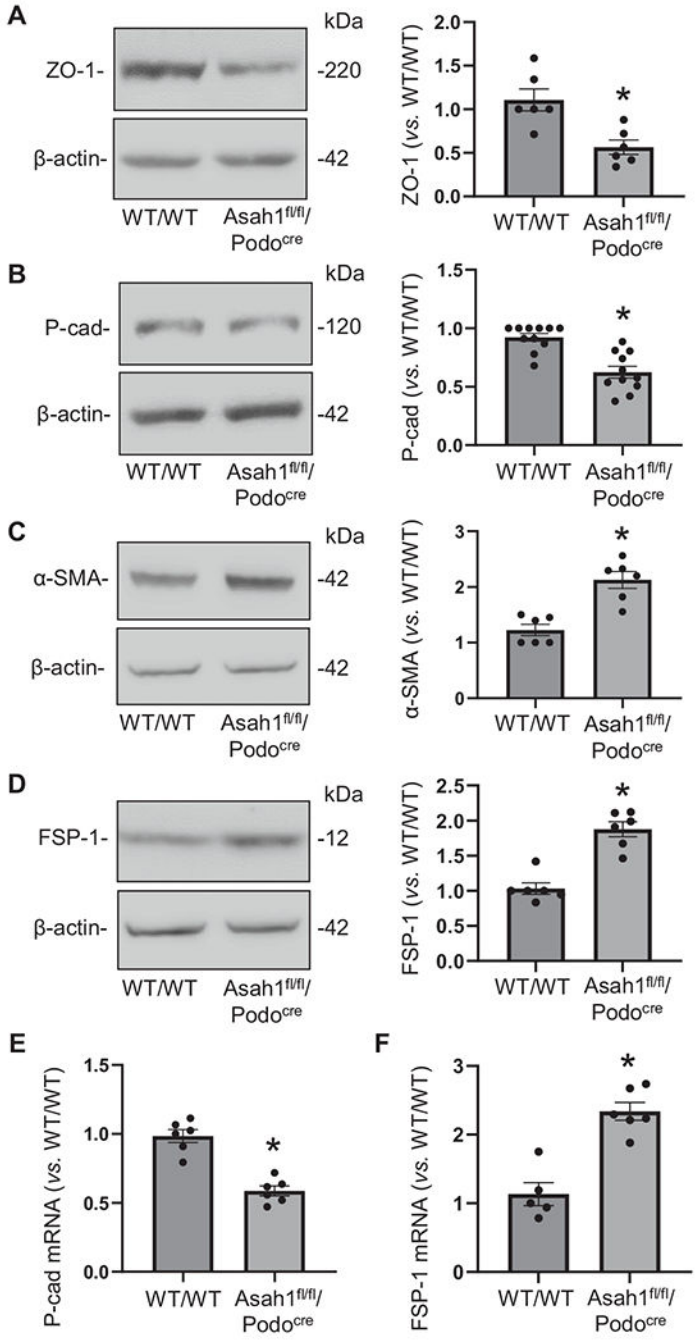

Fig. 5.

Dedifferentiation in podocytes lacking Asah1 gene. A. Representative gel documents and summarized data showing that Asah1 gene deletion significantly decreased ZO-1 in podocytes ($n = 6$). B. Representative gel documents and summarized data showing that Asah1 gene deletion significantly decreased P-cadherin in podocytes ($n = 11$). C. Representative gel documents and summarized data showing that Asah1 gene deletion significantly increased α-SMA in podocytes ($n = 6$). D. Representative gel documents and summarized data showing that Asah1 gene deletion significantly increased FSP-1 in

podocytes (n = 6). E. Summarized data showing that Asah1 gene deletion significantly decreased mRNA of P-cadherin in podocytes (n = 6). F. Summarized data showing that Asah1 gene deletion significantly increased mRNA of FSP-1 in podocytes (n = 5–6). * P < 0.05 vs. WT/WT group.

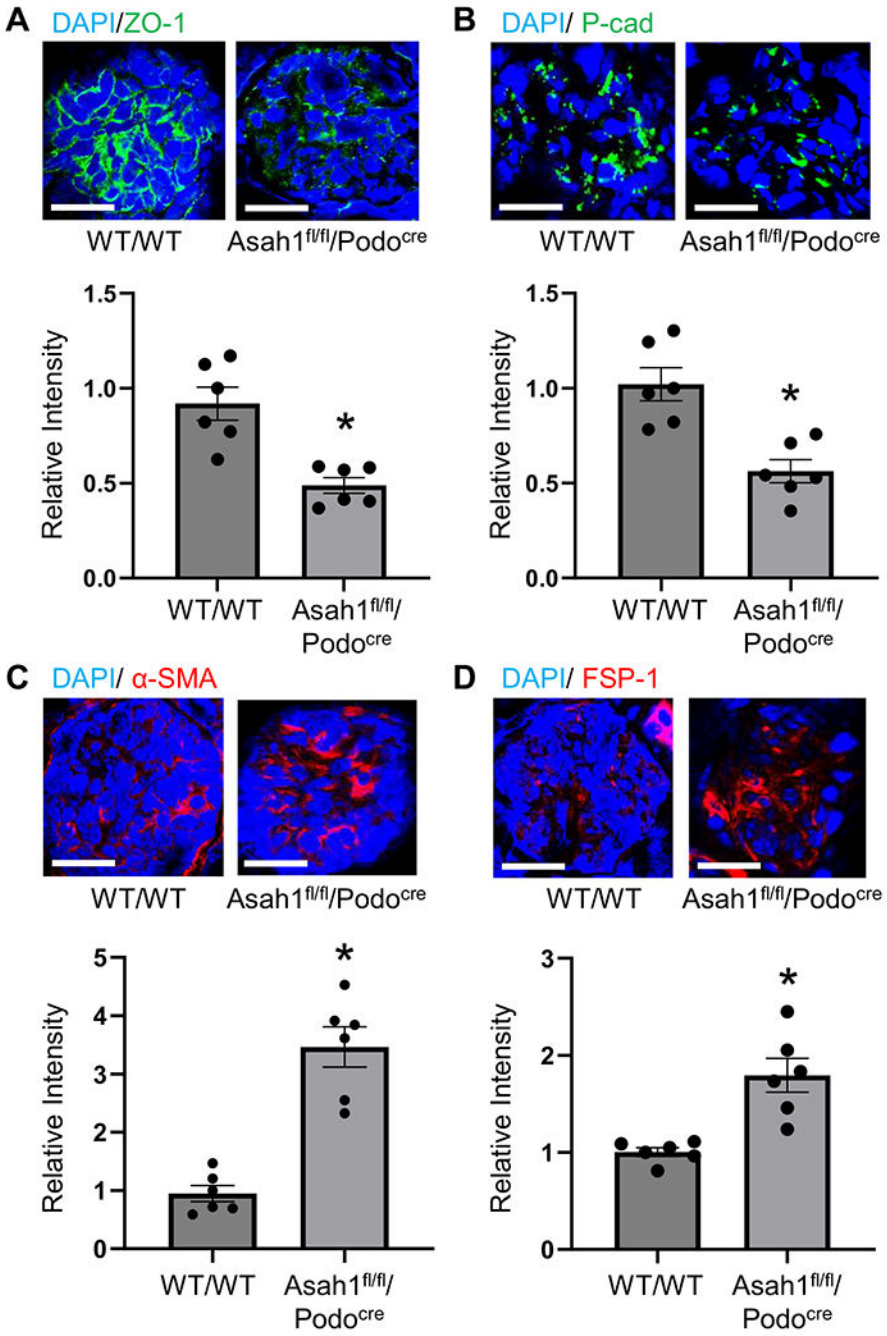

Fig. 6.

Podocyte dedifferentiation in Asah1$^{fl/fl}$/Podo^{cre} mice. A. Representative images and summarized data showing that podocyte-specific Asah1 gene deletion significantly decreased ZO-1 in glomeruli (n = 6). Scale bars = 50 μm. B. Representative images and summarized data showing that podocyte-specific Asah1 gene deletion significantly decreased P-cadherin in glomeruli (n = 6). Scale bars = 50 μm. C. Representative images and summarized data showing that podocyte-specific Asah1 gene deletion significantly increased α-SMA in glomeruli (n = 6). D. Representative images and summarized data showing that

podocyte-specific Asah1 gene deletion significantly increased FSP-1 in glomeruli (n = 6). Scale bars = 50 μm. In the experiments shown in this figure, both male and female mice were randomly assigned into different treatment groups. * $P < 0.05$ vs. WT/WT group.

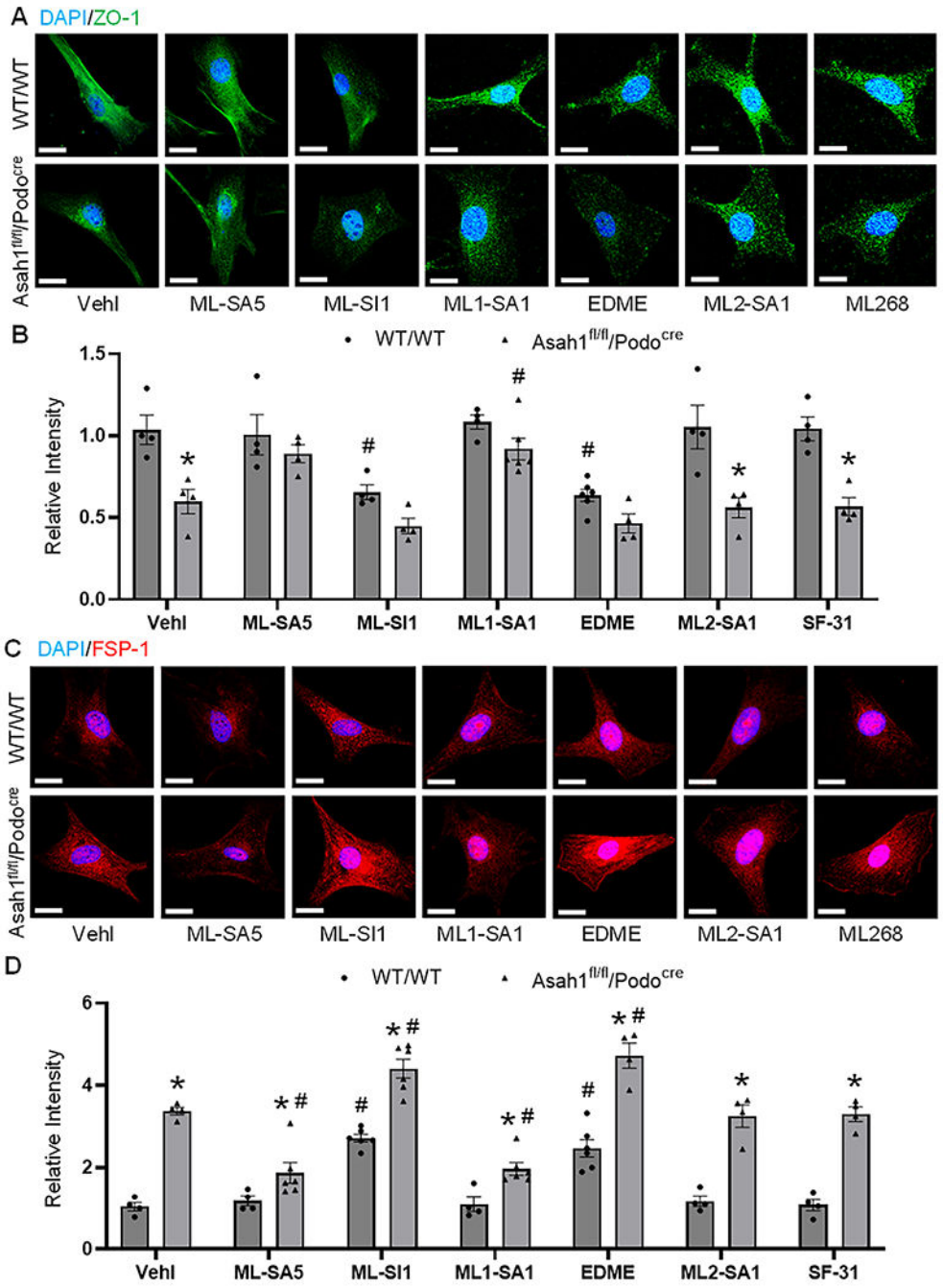

Fig. 7.

Inhibition of dedifferentiation by enhancement of TRPML1 channel activity in podocytes lacking Asah1 gene. A. Representative images showing ZO-1 in podocytes of WT/WT and Asah1$^{fl/fl}$/Podo^{cre} mice under different conditions. Scale bars = 20 μm. B. Summarized data showing ZO-1 in podocytes of WT/WT and Asah1$^{fl/fl}$/Podo^{cre} mice under different conditions (n = 4–6). C. Representative images showing FSP-1 in podocytes of WT/WT and Asah1$^{fl/fl}$/Podo^{cre} mice under different conditions. Scale bars = 20 μm. D. Summarized

data showing FSP-1 in podocytes of WT/WT and Asah1$^{fl/fl}$/Podo^{cre} mice under different conditions (n = 4–6). * P < 0.05 vs. WT/WT group. # P < 0.05 vs. Vehl group.

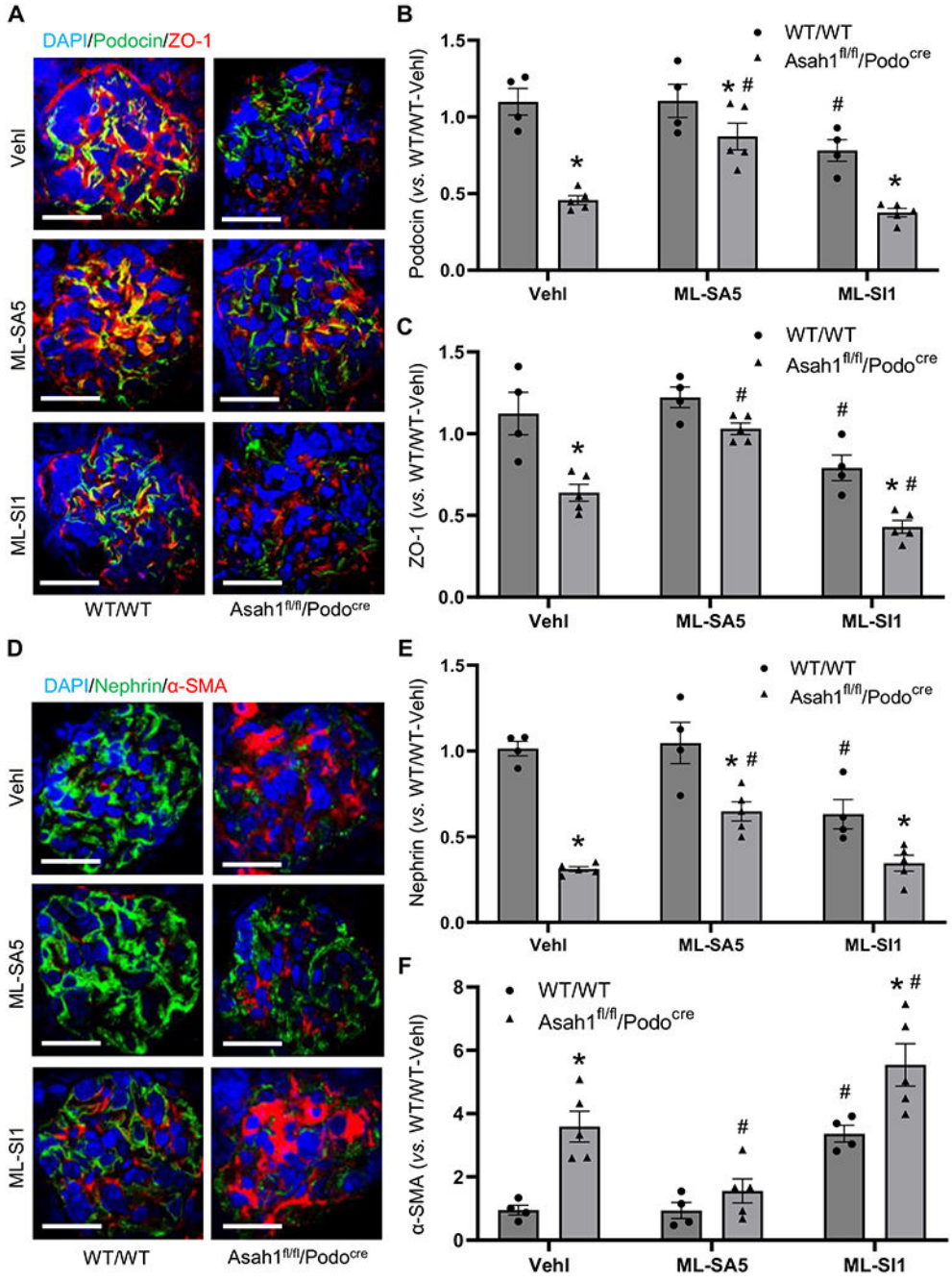

Fig. 8.

Inhibition of podocyte dedifferentiation by activation of TRPML1 channel in Asah1$^{fl/fl}$/Podo^{cre} mice. A. Representative images showing the expression of podocin and ZO-1 in glomeruli of WT/WT and Asah1$^{fl/fl}$/Podo^{cre} mice with different treatments. Scale bars = 50 μm. B. Summarized data showing the expression of podocin in glomeruli of WT/WT and Asah1$^{fl/fl}$/Podo^{cre} mice with different treatments (n = 4–5). C. Summarized data showing the expression of ZO-1 in glomeruli of WT/WT and Asah1$^{fl/fl}$/Podo^{cre} mice with different treatments (n = 4–5). D. Representative images showing the expression of nephrin and

α-SMA in glomeruli of WT/WT and Asah1$^{fl/fl}$/Podo^{cre} mice with different treatments. Scale bars = 50 μm. E. Summarized data showing the expression of nephrin in glomeruli of WT/WT and Asah1$^{fl/fl}$/Podo^{cre} mice with different treatments (n = 4–5). F. Summarized data showing the expression of α-SMA in glomeruli of WT/WT and Asah1$^{fl/fl}$/Podo^{cre} mice with different treatments (n = 4–5). In the experiments shown in this figure, both male and female mice were randomly assigned into different treatment groups. * $P < 0.05$ vs. WT/WT group. # $P < 0.05$ vs. Vehl group.

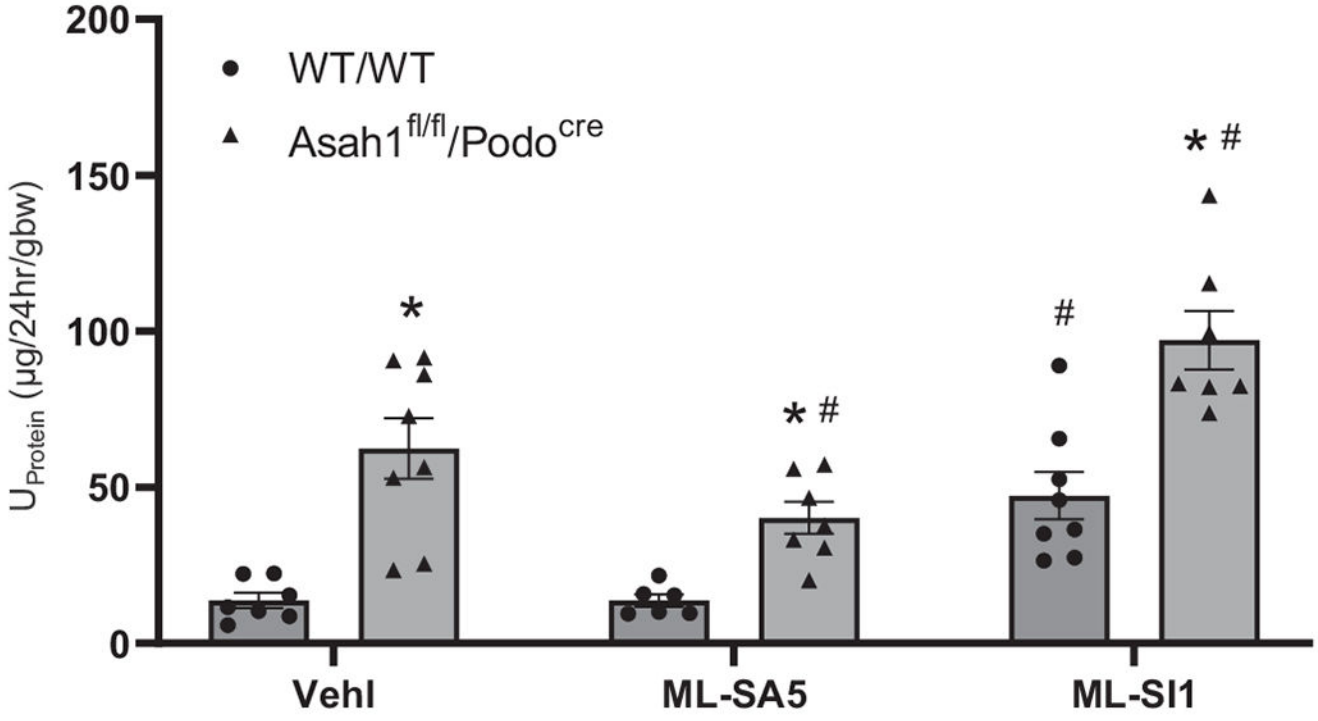

Fig. 9.

Attenuation of proteinuria by activation of TRPML1 channel in Asah1$^{fl/fl}$/Podo^{cre} mice. Urinary protein excretion of WT/WT and Asah1$^{fl/fl}$/Podo^{cre} mice with different treatments. Podocyte-specific Asah1 gene deletion and ML-SI1 significantly enhanced urinary protein excretion. ML-SA5 significantly inhibited urinary protein excretion (n = 6–8). In the experiments shown in this figure, both male and female mice were randomly assigned into different treatment groups. * $P < 0.05$ vs. WT/WT group. # P < 0.05 vs. Vehl group.

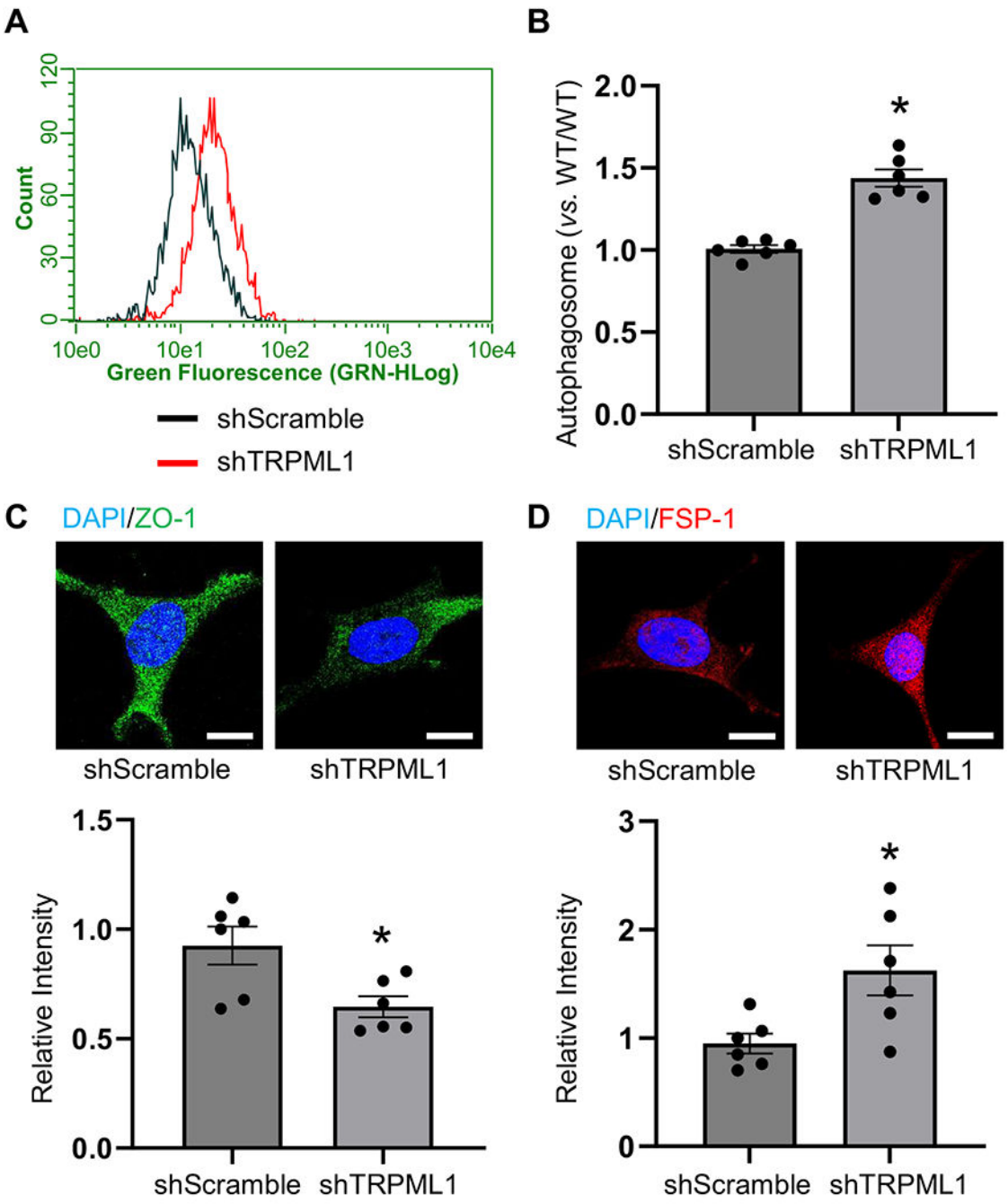

Fig. 10.

Autophagosome accumulation and dedifferentiation in podocytes with TRPML1 gene silencing. A. Representative curves showing the ratio of WT/WT podocytes transfected with scramble shRNA or TRPML1 shRNA with different density of autophagosome. B. Summarized data showing that TRPML1 gene silencing significantly increased autophagosomes in podocytes (n = 6). C. Representative images and summarized data showing that TRPML1 gene silencing significantly decreased ZO-1 expression in podocytes (n = 6). Scale bars = 20 μm. D. Representative images and summarized data showing that

TRPML1 gene silencing significantly increased FSP-1 expression in podocytes (n = 6). Scale bars = 20 μm. * $P < 0.05$ vs. scramble shRNA group.